Kōlams in Graph Theory: Mathematics in South Indian Ritual Art

A Thesis

Presented to

the Faculty of the Department of Mathematics and Statistics

Murray State University

Murray, Kentucky

In Partial Fulfillment

of the Requirements for the Degree

of Master of Science

by

Nathan Hartmann

July 6, 2023

Kōlams in Graph Theory: Mathematics in South Indian Ritual Art

DATE APPROVED: ____________________

____
Dr. Elizabeth Donovan, Thesis Advisor

____
Dr. Robert Donnelly, Thesis Committee

____
Dr. Lesley Wiglesworth, Thesis Committee

____
Dr. Maeve McCarthy, Graduate Coordinator, Jones College of Sci., Eng., and Tech.

____
Dr. Claire Fuller, Dean, Jones College of Sci., Eng., and Tech.

____
Dr. Renee Fister, University Graduate Coordinator

____
Dr. Tim Todd, Provost

Abstract

Kōlams are a ritual art form found in India, most commonly in the southern state of Tamil Nadu. Comprised of different interlocking knots, these women-drawn designs are placed on the entrances to people's home to showcase the household's emotional state and ask the earth goddess Bhudevi for forgiveness. More aesthetically pleasing *kōlams* are considered *latshanam*, where the design permeates beauty; monolinearity is one such aspect that implements *latshanam*. Using graph theory, we examine one style of these drawings, the labyrinthine variety, to identify if a given *kōlam* is monolinear and how to construct monolinear *kōlams*.

Contents

List of Figures

Chapter 1

Introduction

The subject of mathematics is widely considered to be the antithesis of the fine arts, specifically visual arts. Math is seen as a rigid field where only one answer is allowed, but in art, the possibilities are limitless. Despite this uninformed opinion, mathematics and art are more intrinsically alike than most people give credit. Upper level mathematics is more flexible than many perceive, allowing for variety in finding solutions. Furthermore, math can be used to analyze art, identifying designs and how they interact with each other. The mathematical field of graph theory can be used to draw the connections between these seemingly unrelated topics.

In the southernmost state of India of Tamil Nadu, *kōlams* are a ritual art work performed by women and *hijra*, a third gender in Tamil society. Composed of intertwining lines and dot matrices, these designs hold strong spiritual power within Hinduism. One such design is found in Figure 1.0.1. These *kōlams* have innate algorithms and are explored in the field of computer science, yet their mathematical nature does not end in the modern research topic of computer science. Just as graph theory is sometimes understood as a visual math field, *kōlams* are artistic and physical mathematics. Furthermore, *kōlams* can be viewed as a cultural interpretation of graph theory.

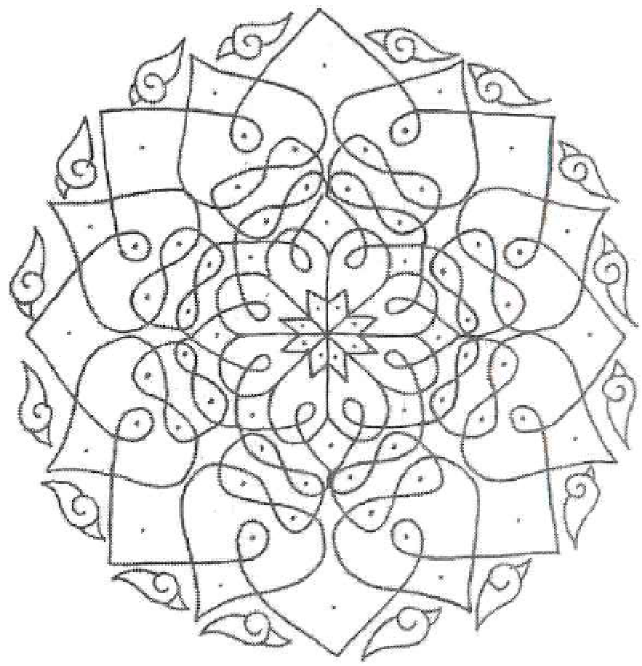

Figure 1.0.1: Lotus and conch in reef knot [16].

To support this claim, we first discuss *kōlams* in depth, including their origins, purposes, and creation in Chapter 2. We conclude Chapter 2 by comparing *kōlams* to related art forms and examining completed research on these other designs. With the cultural relevance of *kōlams*, in Chapter 3 we discuss topological graph theoretic terms and concepts that will aid us when considering these Southern Indian drawings. We merge the above topics in Chapter 4, drawing the connections between graph theory and the *kōlam* tradition.

Chapter 2

Cultural Context

If someone asked whether mathematics and art were similar, most people would answer no. On a base level, most mathematics courses leading up to upper-level theory deal with a systematic way of solving a problem. In calculus, we use derivatives over and over again; algebra uses the same methods when solving for x; and even high school geometry has a large disconnect from art. Most people view them as opposites of thinking. Math is rigid, whereas art is fluid. In art, there is no one solution, while math only has a limited number of correct answers. However, as math courses advance in difficulty, the notion that the field is rigid seems to be incorrect. Artists and mathematicians must be adaptable in their thinking, open to criticisms and change as new thoughts and ideas are introduced.

One of the easiest examples to connect the realms of mathematics and art is the *kōlam*, an art form from the Indian subcontinent that is heavily dependent upon algorithms. In this chapter, we introduce these culturally-rich drawings, as well as their mysterious origins, the historical and modern uses, and highlight similar drawings from all across the globe, ranging from Ireland to Vanuatu in the South Pacific. *Feeding a Thousand Souls* by Nagarajan [14] and Sengupta's *Kōlam Tradition in South India* [16] are the primary sources for the background on *kōlams* in this work.

2.1 *Kōlam* and Its Murky Origins

For roughly 600 years, women from the Southern Indian region of Tamil Nadu have woken up before dawn to prepare their *vāsil pati*, the area in front of their houses, so as to "feed a thousand souls," an important aspect of daily Hindu life. After sweeping the entrances to their homes before the sun rises, women prepare rice flour or stone powder and create elegant drawings on the fresh canvas. These drawings, called *kōlam* in Tamil and other names in various Indian languages and dialects, signify the artist's desires. Some of these various forms include *rangolī* from Gujarat, *muggulu* in Andhra Pradesh and Karnataku, and more across various states in Southern India [16], seen in Figure 2.1.1. *Kōlam*, as Vijaya Nagarajan [14] mentions, are made mostly, though not exclusively, by Hindu women in the Tamil Nadu region as a reminder of the goddess Bhūdevi; "[W]e do everything on [Bhūdevi]...[she has] endless patience." Many women view *kōlam* as delicately as they can, since proficiency in making the pictures is associated with a strong sense of womanliness and ability as a proprietor of the household. The art of drawing *kōlam* is highly stratified by gender; men are quick to dismiss the sheer amount of knowledge and talent that goes into creating them. Even *hijra*, who identify as neither men nor women, have participated in this long-standing tradition.

Although *kōlam* are very traditional, the exact beginnings of this art is hard to pinpoint and sources tend to disagree on the origin of this form. The Tamil word *kōlam* means many things, including beauty, form, and play, so sources tend to argue on when exactly the paintings became a commonality across Southern India. Although sources say that *kōlam* are referenced as early as 300 BCE, many, if not most, agree that roughly 600 years ago is a more conducive starting point, including both researchers Sengupti [16] and Nagarajan [14]. However, the story of one Hindu saint from the 9th century CE, Āntal, greatly mirrors the reasons behind making *kōlam*.

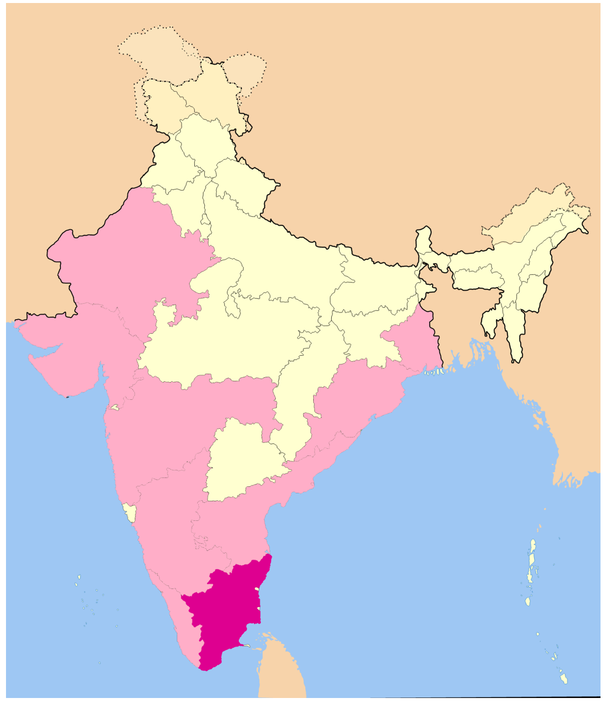

Figure 2.1.1: Map of the states of India, Tamil Nadu in dark pink, other states with *kōlam* equivalents in light pink [1].

As the only female saint of the twelve Vaishnavite saints of medieval Tamil Nadu, Āntal is often recognized for her two song-poems, the *Tiruppāvai* and *Nācciyār Tirumoli*. However, her connection with Vishnu is why she is considered a "key [leitmotif] in women's stories on the origins of the *kōlam*" [14]. As the adopted daughter of a saint, Āntal was tasked with gathering tulasi and flowers every day, with the goal of creating sacred garlands to offer to Vishnu. Even though offerings were for Vishnu and meant to stay away from people to keep pure, she could not resist her admiration with Vishnu. When each garland was complete at the time of offering ceremony, Āntal let her imagination run wild as she imagined she was Vishnu's bride. She did this very often, and her father caught her in the act one day, reprimanding her and withholding the polluted garland from the offering. When Vishnu confronted Āntal's father, Vishnu said that he preferred the flowers Āntal used. After he heard this, Āntal's father began to realize that his daughter was chosen by Vishnu and was therefore an incarnation of Vishnu's wife. For more details regarding Āntal's upbringing and her journey to being a Vaishnavite saint, refer to Chapter 5 of *Feeding a Thousand Souls* [14].

Āntal's deep love and dedication to Vishnu is seen in the second of her aforementioned song-poems, *Nācciyār Tirumoli.* In fact, she even references *kōlams*, using the Sanskrit word *mandala.* This is one of the main reasons for attributing *kōlams* to Āntal. However, Nagarajan provides a more thorough comparison between the two. The art form and Āntal's story both provide elements asking for forgiveness from the gods. In *kōlams*, artists ask for Bhūdevi's forgiveness, but Āntal asked Vishnu for forgiveness. Additionally, the sacred month of Mārkali is the most auspicious time of the year for honoring both; early morning is also the most important time for recognizing both Bhūdevi and Vishnu. In reciting Āntal's poems and drawing *kōlams*, the person starts a conversation with divinity at the beginning of the day, making passersby aware of the grace of gods and goddesses. Although the origins of *kōlam* may not be set in stone, Āntal is one possibility of why *kōlams* are so wide-spread across Tamil Nadu.

Kōlams, despite their murky origins, are intrinsic to culture in Tamil Nadu. A modern retelling of Antal's dedication to Vishnu, the art of Tamil women asks for forgiveness to Bhūdevi while simultaneously fulfilling the aforementioned daily Hindu duty of "feeding a thousand souls." With that goal in mind, there are different occasions when a woman draws *kōlams* outside of the daily activity. Furthermore, the communal nature of the art form leads to a pseudo hierarchy, where certain qualities are emphasized over others.

2.2 Special Occasions and *Latshanam*

Just as the motives behind drawing *kōlam* are tied to the story of the Hindu priest, so is its usage tied to Hinduism. As noted previously, one of the daily rituals of Hinduism is "feeding a thousand souls." This phrase is why the drawings are typically made out of rice flour, allowing the insects to eat it, feeding souls in the process. In *Feeding a Thousand Souls* [14], Nagarajan mentions that the exact amount of beings fed is not of importance, but rather that the artist is nourishing those beings with the daily pictures, blessing all who walk over them.

Because *kōlam*-drawing is a ritual, Nagarajan notes that Tamil women, especially those who practice Hinduism, fulfill their social obligation daily [14]. However, just as with almost – if not, all – religions, special holidays warrant extravagance. Nagarajan mentions that Christian women who accept the mysticism of *kōlams* will create elegant designs on Christmas. However, for Hindu women, Christmas is not the reason many extravagant *kōlams* are made during December and January.

The Tamil month of Margazhi, lasting from mid-December until mid-January, is the most favorable month to create *kōlam*. According to Hindu beliefs, the gods and goddesses roam the earth right before dusk and disappear after dawn during this month. Thus, Nagarajan notes that an observer is likely to see *kōlams* drawn at both dawn and dusk for this reason [14]. Furthermore, Āntal, a key figure to Tamil women and *kōlam*-drawing, is celebrated during Margazhi. Of her two song-poems mentioned in Section 2.1, the first, titled *Tiruppāvai* (translated into English as "Turn Around"), commemorates this month with 30 verses, one for each day of the month. While creating their art, women will recite a verse for the day from this vow song, remembering Āntal and imbuing a stronger auspicious energy into the *kōlam*. Tamil women both in the state and elsewhere continue the tradition with the goal of creating a "shining" *kōlam*, both during the propitious month and not. The festival of Pongal, which occurs during the transition between Margazhi and the next Tamil month Thai, is when most *kōlams* are drawn. During this celebration people hold *kōlam* competitions to gauge who the best is – or rather – whose design is the most *latshanam*.

Latshanam, a romanization of the Tamil word for shining, is a key characteristic of ideal *kōlams*. If someone says that a drawing has *latshanam*, they mean that the inner beauty of the figure permeates the entire drawing. Even if a *kōlam* doesn't shine, the drawing still highlights characteristics of the artist. As a design increases in complexity and detail, observers view its creator as patient with the ability to create beauty around them. Sengupta mentions that skilled women can even create *kōlam* with well over 100 *pulli*, the Tamil word for dots [16]. These two ideas reflect the woman's traditional core, since patience and creative ability are seen as necessary to run a household. Aside from encompassing as many *pulli* as possible, another signifier of *latshanam* is monolinearity, when the *kōlam* is drawn in only one line. Though there are many examples that are not, monolinearity shows a woman's intelligence and dedication [14].

In the hopes of creating *latshanam kōlams*, women not only practice their drawing abilities but also compare their notes with others. Nagarajan writes that finding shining pictures is trial and error, evident in notebooks used for experimenting designs. Since they are shared so frequently, *kōlams* are not known by author but instead by their design. For example, the shield knot *kōlams* seen in Figure 2.2.1 are not known by their original creator(s) but instead by the design referencing a shield. Another prominent design is called Brahma's knot, seen in Figure 2.2.2. Well-known, and even not well-known, designs drawn by creative women lead to variations on them, providing new and interesting figures to inspect and educate.

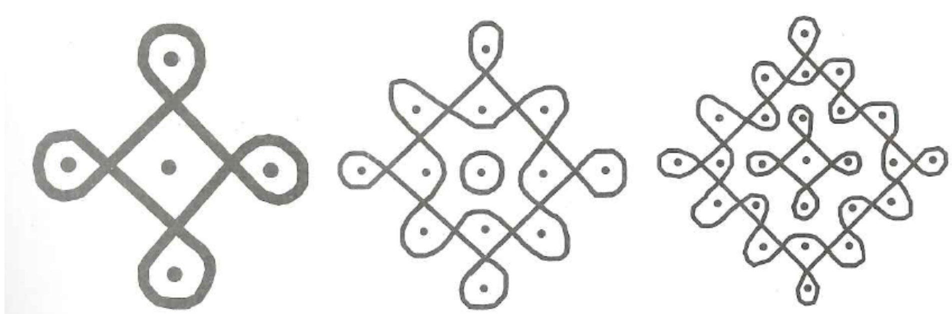

Figure 2.2.1: Different levels of the shield knot, starting with the Nezhi *kōlam* [16].

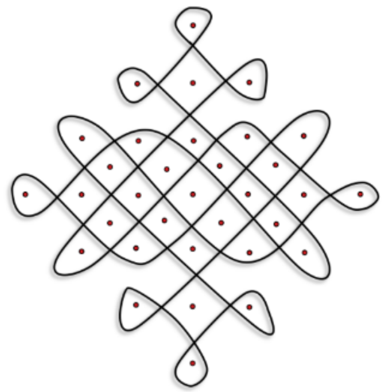

Figure 2.2.2: Brahma's knot [10]

As with all art forms, there is not one be-all-end-all design to follow, even when looking at them. Sengupta broadly categorizes *kōlams* into *kodu* and *pulli*. Figure 2.2.3 shows the two different categories. The former of the two groups, *kodu*, features "geometric design...[using] straight lines often leaving a central area free except for a single dot or with no dot at all" [16]. *Pulli kōlam*, on the other hand, feature numerous dots throughout the design, circumscribed by curving lines. Naturally, these two broad categories lead into smaller and more precise categories, which Sengupta discusses in Chapter 3 of *Kōlam Tradition in South India* [16]. Of the subcategories, variations include concentric squares, interlocking triangles, circles, and even figurative designs [14]. The one type discussed in this paper is the labyrinthine *pulli kōlam*, which is comprised of a square of *pulli* spaced roughly ten centimeters apart, configured in a maze-like shape to indicate transformation, either for those entering the house or those leaving it [16]. The type of *kōlams* this research focuses on is *pulli kōlam*, and the remainder of this work will only consider drawings of that style. Thus, "*kōlam*" will refer only to this style.

Both Nagarajan and Sengupta provide more nuances of *kōlam* design in their respective works, [14] and [16]. However, as with learning an instrument, thoughtful *kōlam*-making comes with time and practice. The next question then is how *kōlams* are created.

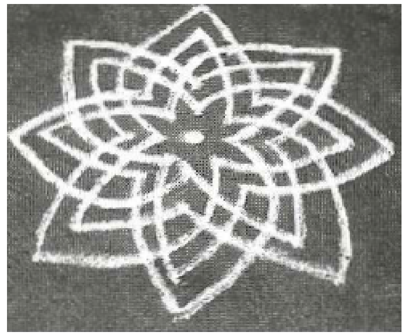

(a) Example of *kodu kōlam* [16].

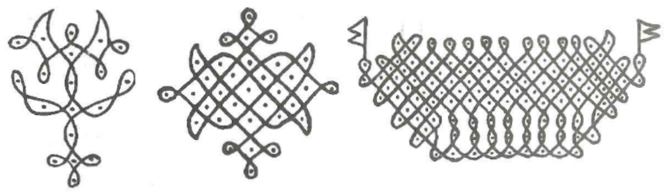

(b) Example of *pulli kōlam* [16].

Figure 2.2.3: Variations in *kodu* and *pulli kōlams*.

2.3 Creating a ***Pulli Kōlam***

Before dawn, women begin their *kōlam*-crafting of the day. Some women opt to draw another *kōlam* at sunset, and this routine is the same. Their canvas, the threshold to the home, needs to be cleaned, regardless of the time of drawing. The artist cleans this area and possibly pours water on the region. This optional preparation step allows the *kōlams* to last longer. After the entire canvas is prepared, the artist is ready to prepare the drawing instrument: not a paintbrush nor a pencil, but powder. Although rice flour is most commonly used, stone powder, a cheaper alternative to the relatively expensive flour, also provides the same results. After both the canvas and the powder or flour are ready, the artist can begin their work for the day.

Beginning by creating a large array of dots, the woman draws a number of *pulli* in columns and rows spaced evenly apart. This matrix of points on the ground mark the location of the *kōlam*. Figure 2.3.1a shows the *pulli* all spaced roughly ten centimeters apart, which follows the standard. Depending upon the artist and the desired *kōlam*, the dots will either be circumscribed or connected. For *pulli kōlam*, the artist draws the lines to weave around the points on the ground. Figure 2.3.1b shows the start of this process. Memorizing a pattern from her notebook, the woman copies her design, ensuring that each line she creates begins and ends at the same point, forming closed curves. Once one line is completed, should the design warrant multiple lines, the remaining lines are made one at a time with the goal to finalize the designer's vision and match their memory. Although the word "line" is used, in a *kōlam*'s design these lines act similarly to *sona*, as Chavey [6] shared. To summarize Chavey and apply it to the Indian art form, the *pulli* drawn identify natural boundaries for the *kōlam* to exist. The lines of the art use these boundaries, smoothly curving as the line approaches them. Figure 2.3.1c shows the details of a finalized *kōlam* with 100, 000 *pulli*.

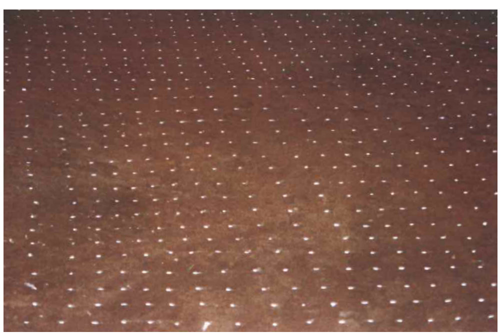

(a) Details of *pulli* arrangement [14].

(b) The beginnings of a *kōlam* [16].

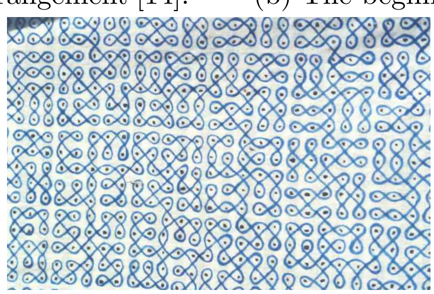

(c) Details of a *kōlam* with 100, 000 *pulli* [14].

Figure 2.3.1: Steps of *kōlam*-making.

As she draws the *kōlam*, the artist follows a few conventions. Adapting this list from Ishimoto [12] and Gopalan [10], and using the social criteria provided by

Nagarajan [14] and Sengupta [16], there are rules guiding the *kōlam*'s composition. The rules are as follows:

Rule 2.3.1 (*Kōlam* Crafting Rules – Adapted from [12] and [10].)**.**

1. All *pulli* should be circumscribed.

2. Every *pulli* must be isolated from another. One *pulli* is allowed in each empty space between lines.

3. Each line in the *kōlam* must be closed.

4. Only one circumscription of a line is allowed to encompass each *pulli*. We cannot circle around a *pulli* multiple times.

5. Each line circumscribing a dot should do so via a teardrop, a lens, a partial stadium, a fan, or a square.

6. The *kōlam* should retain some form of symmetry, either through a reflection or a rotation.

In our to come to a more sound understanding of each rule, there is further elaboration on each, even those that are easier to understand. To satisfy the fifth of these rules, various shapes must circumscribe the *pulli*. Elaborating on the shapes used to circumscribe, some are easier to recognize, but each of the five shapes have importance in the overall design of the *kōlam*. A teardrop, a lanceolate with one pointed end seen in Figure 2.3.2a, is the shape that loops around the cardinal pulli in the drawing. The direction of the teardrop is indicated by the direction the point of the teardrop is facing. A lens is a two-sided circular shape, similar to the intersection in a Venn diagram as in Figure 2.3.2b. A stadium is a rectangle with two semi-circles attached on opposite ends, as seen in Figure 2.3.2c, and we consider the partial stadium as a rectangle with one semi-circle on an end, depicted in Figure 2.3.2d. A fan, also known as a sector of a circle and found in Figure 2.3.2e, is a three-sided shape where two straight sides are of equal length and the remaining side is the arc of a circle connecting the two. Diamonds have sides of equal length and are rotated so that the corners face the cardinal directions. Figure 2.3.2 shows what each of these shapes look like isolated, in the orientation they might appear in the *kōlam*. In short, once all *pulli* are circumscribed sufficiently as desired, the drawing is done. To help understand what is occurring, *pulli* will always be colored red.

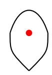

(a) A down-facing teardrop.

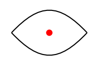

(b) A (horizontal) lens.

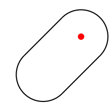

(c) A full stadium with a *pulli* inside.

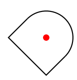

(d) A partial stadium.

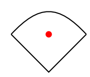

(e) A downward-facing fan.

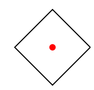

(f) A diamond.

Figure 2.3.2: Six shapes used to circumscribe *pulli*.

With the *kōlam* finished, its spiritual abilities start, and the task of feeding of a thousand souls commences. The drawings bless those who walk over them, wiping away the figures throughout the day. All that interact with the figure, human or not, are blessed from the gods as they passively act in the ritual. Nagarajan mentions that around noontime the flour designs are faded away from passersby. When the sun is setting, women start this whole process over again. They sweep the thresholds, gather their flour or powder, and draw a *kōlam* for the nighttime [14]. In completing this ritual daily, women keep their karma in balance.

Kōlam-crafting is intention; each movement the artist makes is highly calculated and highly meaningful. In Tamil culture, *kōlams* express the mental state of the artist. The artist shows birth, marriage, and various stages of life. Furthermore, the absence of a *kōlam* indicates a somber event such as death has occurred in the household. These figures show just a fraction of the culture of Tamil Nadu, hopefully providing a sense of what happens in the background of *kōlams*, the religious intention, the mental state of the artist, and even the state of all members of the household. As we travel outside of Tamil Nadu, we see similar figures, stretching around the globe from Celtic cultures to African ones and even different peoples in the South Pacific.

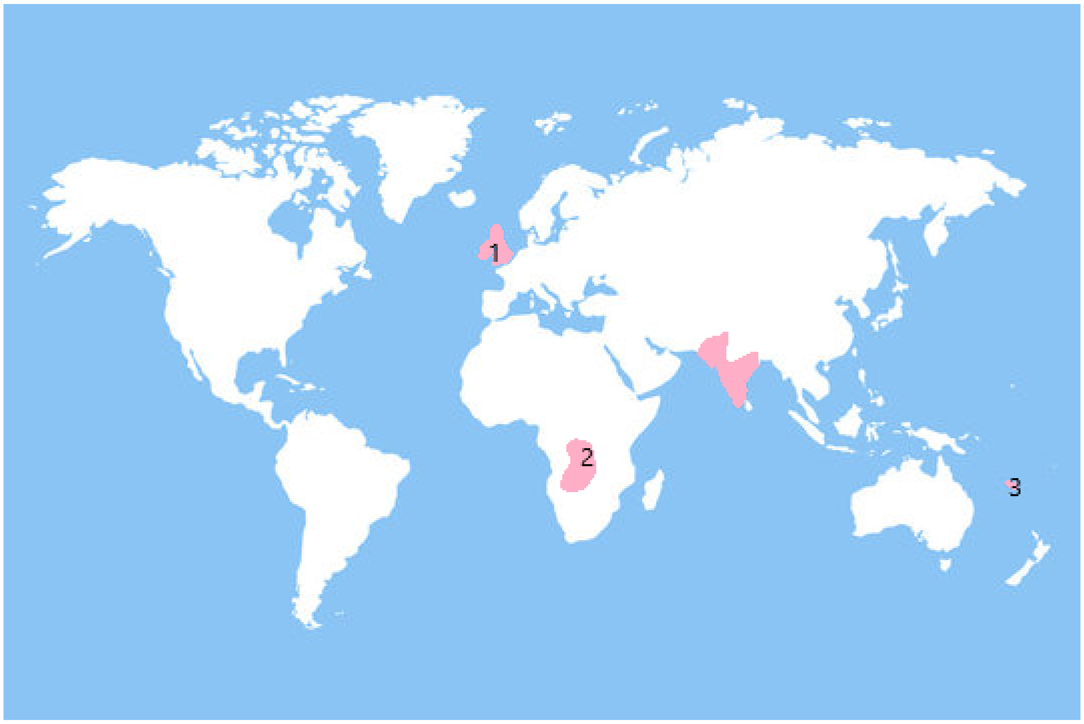

Figure 2.3.3: Map of world with different *kōlam*-related designs in pink. 1: Celtic knots, 2: *Sona*, 3: *Nitus*, unlabelled: *Kōlams*.

2.4 Cross-Cultural Encounters

Kōlams, in their exact form, are unique to Southern India, but similar figures exist elsewhere. See Figure 2.3.3 to see four regions where *kōlams* and similar art forms can be found. These comparable art forms, especially those that have been examined in more depth than *kōlam*, aid in the analysis of the Southern Indian figures. One similar form of drawing is that of Celtic knots. The Celtic "interlaced patterns," as Sengupta shares, have origins in the Roman Empire during the third and fourth centuries, and interlaces are even seen within Byzantine architecture, Medieval illumination, Coptic, Ethiopian, and Islamic art [16]. Despite possessing a written history that survived time, Celtic knots differ from *kōlams* in two key ways. Firstly, they lack *pulli* or any equivalent dots in the empty spaces. Next, the Celtic knots are drawn on rectangular grids [11]. In application, Celtic knots are used for protection just as *kōlams* are. Figure 2.4.1 shows two different variations of Celtic knots.

(a) Celtic knot [11]. (b) A rectangular Celtic knot [8].

Figure 2.4.1: Two Celtic knot variants.

Celtic knots are not the only art form using these interlocking twists, nor is protection the only use for these art forms. Located in Central Africa, the Tchokwe people also draw weaving lines in a similar fashion called *sona*. Compared to both Celtic knots and *kōlam*, *sona* contain elements to both art forms. Specifically, the men-drawn, story-telling *sona* use a matrix of dots, much like the Tamil art [3]. However, instead of having a scalable size, the drawn matrix does not need to be a specific shape. Furthermore, circumscribing dots is not a requirement, as the dots become either "interior" or "exterior" to the lines drawn, aiding in storytelling. Figure 2.4.2 shows the variety in the Tchowke designs.

Storytelling is not the only boon provided of these similarly-drawn figures. Travelling to the South Pacific to Malekula, an island in Vanuatu, *nitus* can be seen. *Nitus*, the sand drawings found here, are used in death ceremonies, granting the deceased passage into the Land of the Dead [2]. A *hi*, a turtle *nitu*, can be seen in Figure 2.4.3. The Vanuatu variants of these drawings are similar to the *sona*, despite needing symmetry like *kōlam*. Dots are not used for all figures, and those *nitus* that have dots are

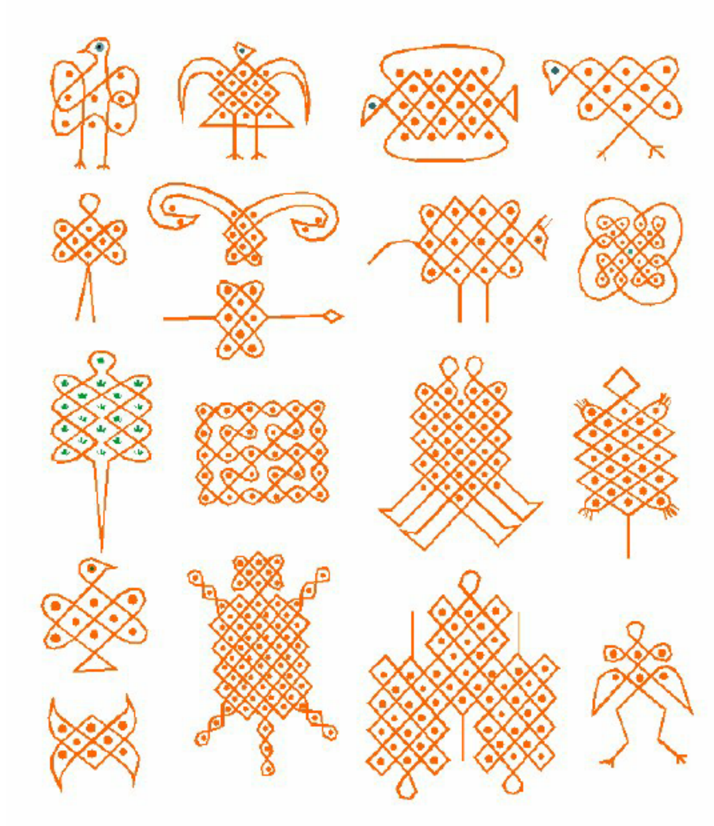

Figure 2.4.2: Many *sona* examples [15].

treated the same as in *sona*, either outside or inside the drawn lines, each conveying an underlying message.

Whether they ask for forgiveness, provide protection, tell a story, or send on the deceased, *kōlam* and the similar art forms are seen through many cultures, many of whom seem entirely unconnected otherwise. Despite this, similar mindsets are used when crafting. No matter who the specific creator was, each person had to consider how one small choice would affect the whole figure. Algorithms and inventive mathematical thinking give way to these unique drawings.

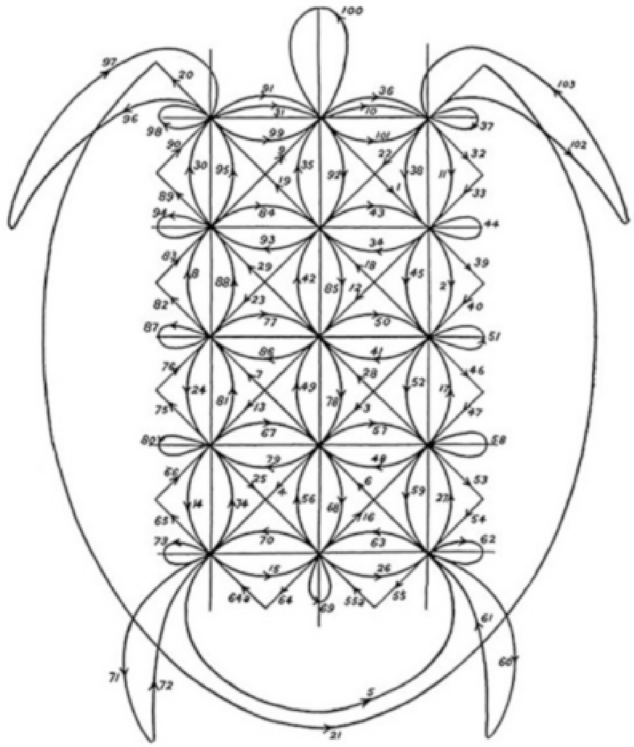

Figure 2.4.3: *Nitu* example, showcasing direction when drawing [17].

2.5 Mathematical Research on *Kōlam* and Similar Art

Since *kōlams*, as well as *sona* and *nitus*, have entered the global eye only recently, very little research has emerged on the mathematical complexities of these line drawings. That being said, ethnomathematician Marcia Ascher has formed a foundation for the mathematics behind *kōlam*. In *Mathematics Elsewhere* [4], Marcia Ascher describes some of the algorithmic processes in creating some *kōlam*, using string language. In denoting which direction the line goes and the angle the line curves, she gave an understanding of how repeated patterns in the Southern Indian art can be described without words. Additionally, her findings gives a way to interpret how a *kōlam* with a repeated pattern can be made if said pattern is repeated any number of times.

Outside of the ethnomathematic perspective, *kōlam* are highly intriguing to computer scientists. Yukitaka Ishimoto viewed *kōlam* under the pretext of knot theory, interpreting *kōlam* forms given a diamond-shaped grid, and generalizing them to their idea of an "Infinite *kōlam*" [12]. His goal was to find the number of *pulli kōlam*, given a certain amount of dots in a configuration. Additionally, creating *kōlam* has been the goal of computer scientists and mathematicians alike. Using topology to create *kōlam* of any size, Venkatraman Gopalan and Brian VanLeeuwen proposed a five-step approach to systematically draw a *kōlam* with N dots in any configuration [10]. Though there is research in the Tamil designs, their Celtic counterparts have been studied more. Gross and Tucker [11] viewed the Celtic drawings from a knot theory perspective, finding a correspondence between Celtic knots and alternating links. Connor and Ward [7] used Celtic knots to showcase how knot theory works. The investigations of these varieties of design do not end here, however. Using *sona*, Chavey [6] gives an understanding of how various forms of mathematical induction work. The *kōlams* of Tamil Nadu provide just as much relevance to the mathematical community as its related art forms.

The history of *kōlam* is rich, full of mystery and religion. Though its origins remain partially unknown, Tamil women show that their ritual art connects many seemingly unrelated fields. Art, religion, mathematics, and other fields unite in the *kōlams* of each and every woman that draws one; all of the subjects are intrinsic to the drawings. In the next chapter, we introduce graph theoretic concepts that we will in turn apply to *kōlam*, showing that these figures are inherently mathematical.

Chapter 3

Graph Theory Terminology

To aid our search of determining when *kōlams* are monolinear, we utilize graph theory. In this chapter, we discuss the graph theoretic concepts we need for our analysis. After identifying core ideas, we shift into topological graph theory to gain the depth and connections necessary for our work.

3.1 Basic Terminology

We begin our terminology overview with the elements that comprise a graph: vertices and edges.

Definition 3.1.1. A **graph** G is an ordered pair $(V(G), E(G))$ comprised of two sets, the vertex set and edge set. The **vertex set** $V(G) = \{v_0, v_1, \ldots, v_n\}$ is the set of all vertices of G. The **edge set** of G, $E(G) = \{(v_i, v_j) \mid v_i, v_j \in V(G)\}$, is the set consisting of the unordered pairs of vertices such that there is an edge between vertices v_i and v_j.

Graphs highlight how items, often depicted as vertices, are related. These relationships are seen as the edges connected vertices. For any graph, there is no limit to the number of vertices or edges. However, in our work we assume that all graphs will contain a finite amount of both vertices and edges. Additionally, we allow multiple edges between vertices and loops, edges that start and end at the same vertex. Furthermore, we can traverse these graphs, showing further relationships between vertices. One such traversal is by paths, which we go on to define.

Definition 3.1.2. A list of vertices, $u = w_1, \ldots, w_k = v$, of a graph G is a u, v-**walk**. When $u = v$, the walk is considered **closed**. If each vertex is distinct in a walk, the walk is instead called a u, v-**path** If a path's endpoints are the same, then the path called a **cycle**.

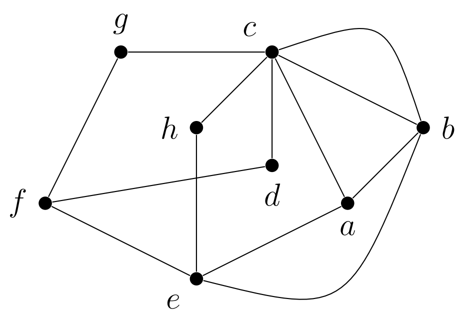

Figure 3.1.1: An example of a graph, G.

Figure 3.1.1 gives us an example of graph that contains many cycles and paths. In fact, the walk c, a, e, f, d, c is a cycle, and c, g, f, e, b, a is a path in this cycle in the given graph G. Paths and cycles are integral parts of graphs that help identify innate connections between vertices. Next, we discuss degree.

Definition 3.1.3. The number of edges incident to a vertex $v \in G$ is the **degree** of v, written as $d(v)$. If all vertices have degree k, then the graph is k-**regular**.

Identifying degrees in a graph G can help us learn more about G itself. From Figure 3.1.1, we can see the degrees of each vertex of the graph. Thus, $d(c) = 6$, $d(b) = d(e) = 4$, $d(a) = d(f) = 3$, and $d(g) = d(h) = d(i) = 2$. Figure 3.1.2 shows two examples of variations in 2-regular graphs. In the examples provided, we see the next topic of discussion, what it means for a graph to be connected.

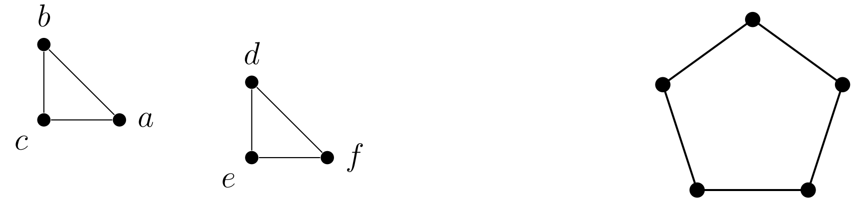

(a) A disconnected 2-regular graph. (b) A connected 2-regular graph.

Figure 3.1.2: Variations in 2-regular graphs.

Definition 3.1.4. For a graph G, if there exists a path between any two vertices $u, v \in v(G)$, then G is a **connected** graph. On the other hand, if there exists a $u, v \in V(G)$ such that there is no path between the two, then G is called **disconnected**. If a graph is connected and contains no cycles, then the graph is a **tree**.

As mentioned in Figures 3.1.2a and 3.1.2b, we see some differences in disconnected and connected graphs. Disconnected graphs will always be comprised of disconnected subgraphs called components, and connected graphs will always contain a single component. Additionally, Figure 3.1.4 showcases a tree. We next pose the question of how to disconnect a connected graph. We start by finding subgraphs.

Definition 3.1.5. If a graph H has vertices $v_0, v_1, ..., v_k$ and edges $e_0, e_1, ..., e_m$ that all belong to a graph G, then H is a **subgraph** of G, and $H \in G$.

Figures 3.1.3a and 3.1.3b depict a graph and one possible subgraph. Vertices of a subgraph do not need to have all the edges present in the base graph nor do all vertices of a graph need to be present in the subgraph. As we can see in Figure 3.1.3, five vertices of G are not present in H. Additionally, two edges, namely ef and jk do not exist in H either. Should those two edges be in the subgraph, H would have been considered an induced subgraph. We more formally define induced subgraphs.

Definition 3.1.6. Let G and H be graphs such that H is a subgraph of G. H is an **induced subgraph** if and only if all edges in $E(H)$ also exist in $E(G)$.

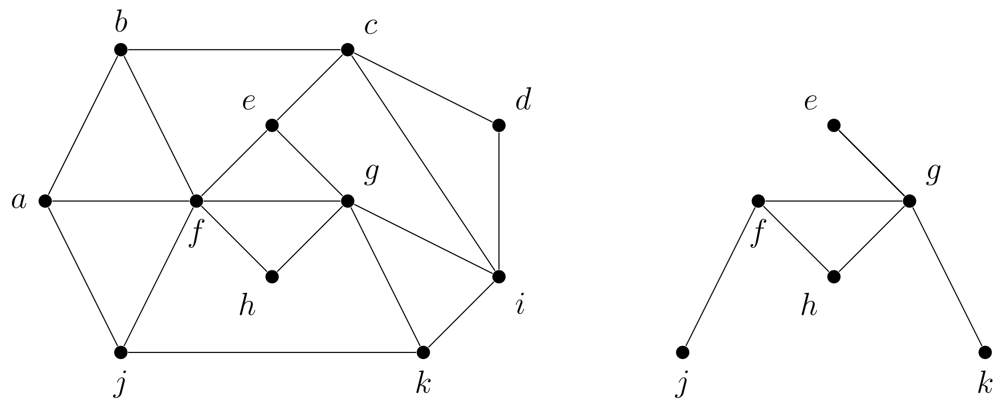

(a) Graph G. (b) Subgraph $H \subset G$.

Figure 3.1.3: A graph and a subgraph.

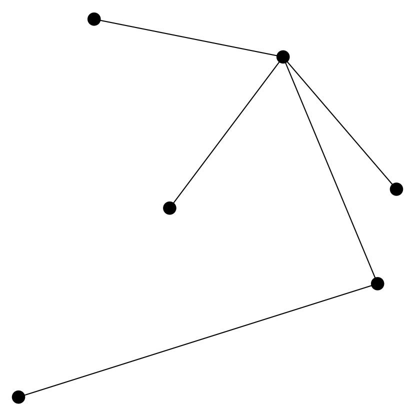

Figure 3.1.4: A tree, T.

Definition 3.1.7. If the deletion of an edge $e \in E(G)$ disconnects G, then e is a **cut-edge**. Likewise, if the removal of a vertex $v \in V(G)$ disconnects G, v is a **cut-vertex**. If a maximally connected subgraph G has no cut-vertex, then G is considered a **block**.

We can identify the cut-edges and cut-vertices from Figure 3.1.5a and even see how their deletion affects the graph as a whole in Figures 3.1.5b and 3.1.5c. When removing a cut edge, we only remove the edge. However, when we remove a cut-vertex, we also eliminate all edges incident to said vertex. Every edge in a tree is a cut-edge, and all vertices with degree 2 or larger in a tree are cut-vertices. We can reexamine Figure 3.1.4 to help convince ourselves of this fact. The last topic we will mention before going into topological graph theory is the notion of subgraphs.

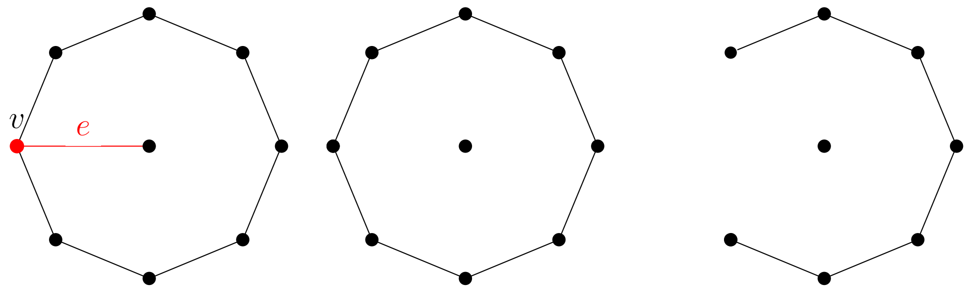

(a) Graph G (b) $G - e$ (c) $G - v$

Figure 3.1.5: Effects of cut vertices and cut edges in graphs.

Now that we have a general understanding of basic graph theory terms and ideas, we shift our focus over to topological graph theory.

3.2 Topological Graph Theory

Thus far, we have only discussed graph theory in terms of general spaces. We can place our graphs in any space, such as a 3-dimensional curved plane. An example of a graph in such a plane is seen in Figure 3.2.1. Although we can place graphs in higher dimensions, the graphs we will encounter will be placed in 2-dimensions for simplicity's sake. Figure 3.2.2 shows the same graph in a plane, oriented in 3 different ways. Notice that in each of the four visualizations of the graph, the interactions between vertices through edges remain the same. Vertex a is always has degree 3 and is adjacent to vertices b, d, and e. Even if these visualizations all refer to the same graph, we try to minimize the number of times edges overlap, which aids in legibility. We aim to make our graphs planar, which we define.

Definition 3.2.1. A graph G that is drawn such that its edges only intersect at the vertices is called a **planar** graph.

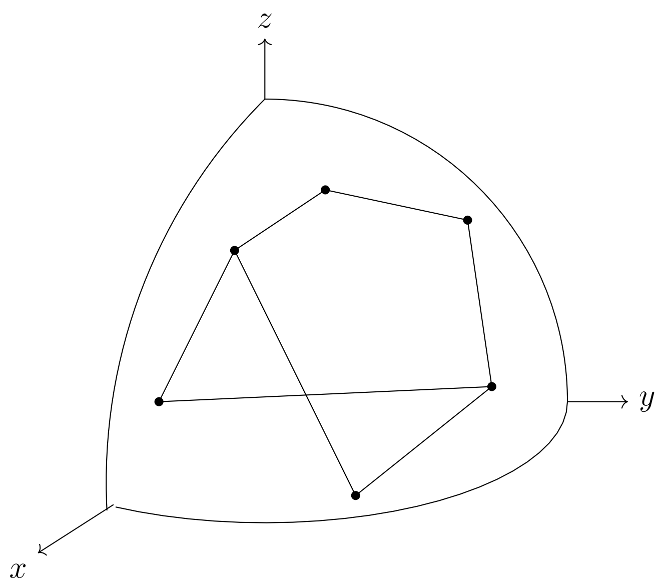

Figure 3.2.1: A graph G, located on a curved 3-dimensional plane.

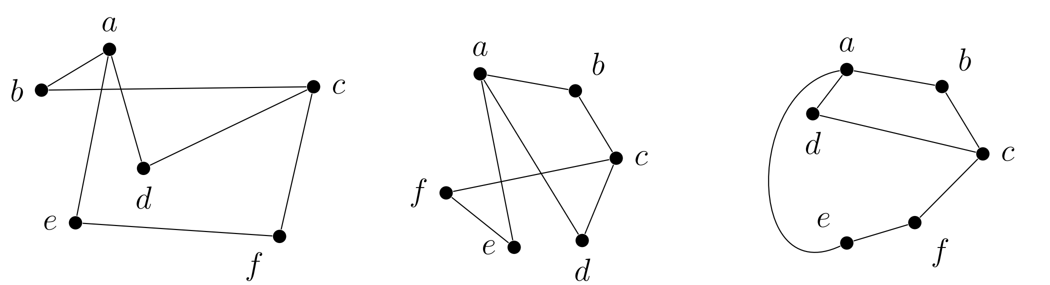

(a) G in a 2-dimensional setting. (b) G in a different 2-dimensional orientation. (c) G in a planar construction.

Figure 3.2.2: Variations of G embedded in 2-dimensional settings.

Figure 3.2.2c shows a planar embedding of our aforementioned graph G. Planar graphs provide more insight about a specific graph, especially when regarding relationships. Thus, we will only consider planar embeddings for graphs for the remainder of this work. Thus no edges will cross over another in our constructions. Beyond vertices and edges, planar graphs also result in faces, which we define next.

Definition 3.2.2. A region in a graph G that is bounded by a set of vertices and edges is a **face**. We denote the set of all faces in G as $F(G)$.

Figure 3.2.3 shows the faces of the graph, colored red, pink, and white. Note that

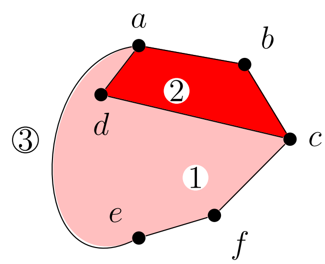

Figure 3.2.3: Planar graph G with the three faces colored and numbered.

the exterior of the graph is also a face, extending as far as the graph's placement will allow. As alluded, one of the numerous things we can do with these faces is separate them into groups by coloring them.

Definition 3.2.3. A **k-face-coloring** is a labeling $\varphi : F(G) \to T$, where $|T| = k$. A **perfect k-face coloring** occurs when no face of a color is next to another face with the same color.

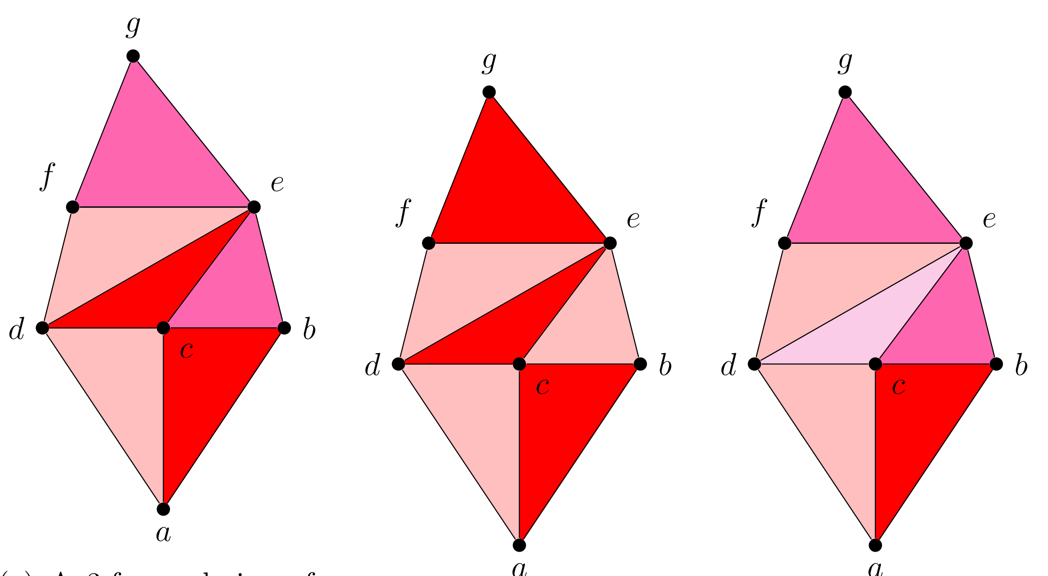

(a) A 3-face coloring of a graph G.

(b) A 2-face coloring of G.

(c) A 4-face coloring of G.

Figure 3.2.4: Graph G with various face colorings.

Figures 3.2.4 shows three alternative face colorings for a graph G. However, when considering colorings, we typically want to find the minimum number of colors necessary for a perfect coloring. Figure 3.2.4b shows this minimum face color number to be two. With all of this, let us instead shift our focus from graphs very briefly to discuss knot theory, which will aid us later.

3.2.4 Knot Theory

We shift our focus from specific embeddings of graphs to the notion of knot theory.

Definition 3.2.5. A **knot** is a piecewise linear closed curve in $\mathbb{R}^3$. The collection of one or more pairwise disjoint knots is known as a **link**.

Since showing three dimensions is difficult on paper, we often embed links and knots in $\mathbb{R}^2$ in the form of a **link diagram**. In these link diagrams, we do not indicate the direction of crossings, specifically the over and under directions. We can derive graphs from the link diagram, which we call shadow graphs.

Definition 3.2.6. For a link L expressed as a link diagram, we can define the **shadow graph** of L, $\mathcal{S}_L$, by its vertices and edges. A vertex $v \in V(\mathcal{S}_L)$ is located where a crossing in L is. An edge $v_i v_j \in E(\mathcal{S}_L)$ exists if and only if there is a curve connecting two crossings v_i, v_j.

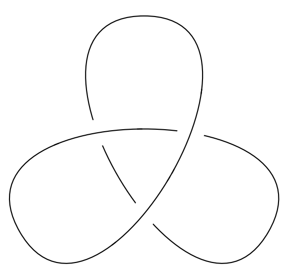

(a) An example of a link L.

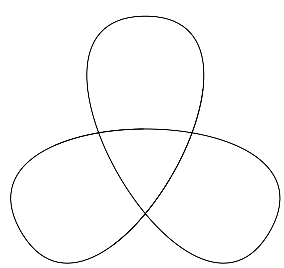

(b) L as a link diagram.

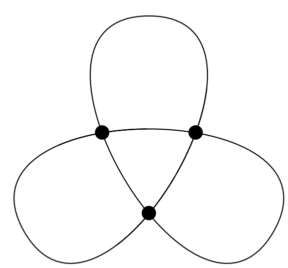

(c) $\mathcal{S}_L$, the shadow graph of L.

Figure 3.2.5: A link, link diagram, and its shadow graph.

Figure 3.2.5 shows the relationship between a specific link, its link diagram L, and its shadow graph $\mathcal{S}_L$. Since we will consider knots from a graph theory perspective, our focus will be more on shadow graphs than links and link diagrams. As such, when considering a shadow graph, if the link is understood from the context, we omit the subscript, identifying the shadow graph as $\mathcal{S}$. There are, of course, many interesting features of shadow graphs. One such attribute is that any $\mathcal{S}$ is a 4-regular planar graph, meaning that each shadow graph has a perfect 2-face coloring. Figure 3.2.6 showcases one such perfect 2-face coloring. However, this raises a new question: Are there other ways to interpret this graph? Let's explore one possibility using walks.

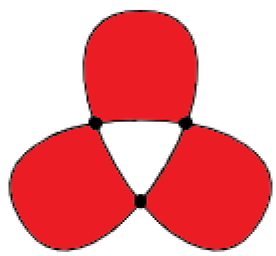

Figure 3.2.6: 2-face coloring of $\mathcal{S}_L$.

We use the idea of left-right walks, adapted from Godsil and Royle [9], which are defined as follows. Replace each vertex with a disk of radius $\varepsilon_v > 0$ and redraw each edge with width ε_e, with $0 < \varepsilon_e < \varepsilon_v$, as seen in Figure 3.2.7a. In the middle of each edge, we "pinch" the edge, forcing both sides to converge to a single point. Figure 3.2.7b shows how the graph will look after this operation. We can "traverse" the new graph by left-right walks, starting at one side of a disk-vertex, walking along its boundary until an edge is reached, and then continuing the traversal along the side of this edge. Upon arriving at the point in the center of the edge, we move to the opposite side of the edge and continue the traversal until we reach the next vertex. We then proceed to walk along the boundary of the disk-vertex until the side of another edge is reached. This process is continued until we return to our starting point, making a closed walk—one that alternates between the left and right sides of the traversed edges. We repeat this process until we have traversed over both sides of each edge. As previously noted, this process of left-right walks can be performed on any shadow graph $\mathcal{S}$. For legibility in our drawings, we smooth the edges to appear less jagged, resulting in Figure 3.2.7c.

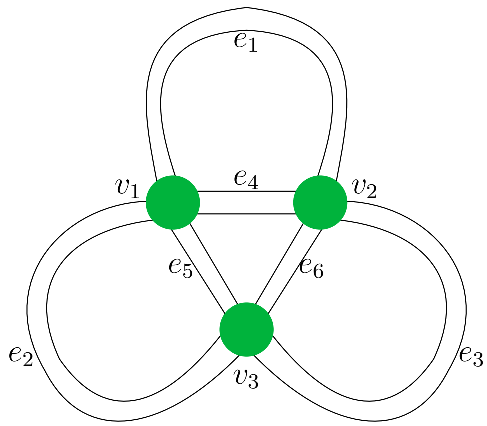

(a) Replacing vertices and edges step of left-right walk process.

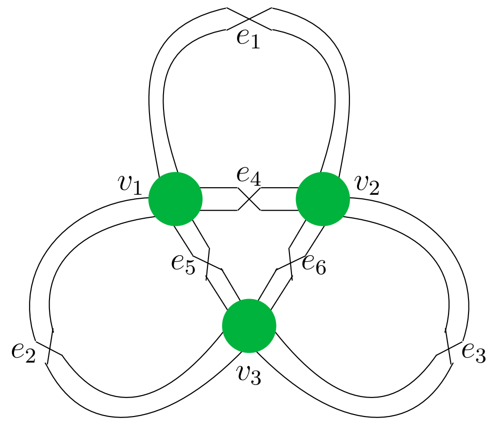

(b) Pinching edges step of left-right walk process.

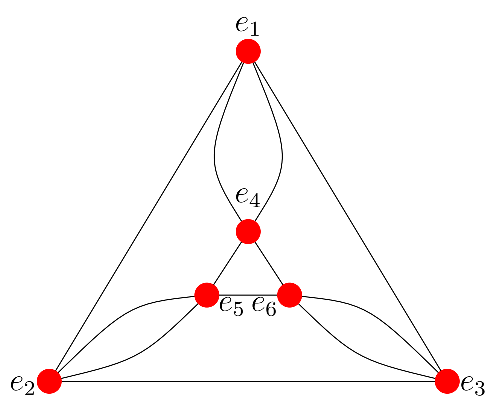

(c) Tracing the graph in left-right walks.

Figure 3.2.7: The left-right walk process on shadow graph G.

Contrasting the process for walks, we find left-right walks specifically by writing a list of vertices and edges. Using the "pinched" graph, we can find a walk in Figure 3.2.7b by writing a list of vertices and edges we traverse. We find that there are three distinct left-right cycles in Figure 3.2.7b, namely $v_1, e_1, v_2, e_4, v_1, e_5, v_3, e_2, v_1$; $v_1, e_1, v_2, e_3, v_3, e_6, v_2, e_4, v_1$; and $v_3, e_5, v_1, e_2, v_3, e_3, v_2, e_6, v_3$. Note that the first two of these cycles start with the same three elements. Despite this, these cycles use the two different sides of the edge e_1, which control the second traversed edge in the cycle. Instead of viewing this graph with its left-right walks, we can redefine the graph, replacing the cross-over points with vertices. We call this graph the medial graph, defined as follows.

Definition 3.2.7. Given a connected planar graph G, the **medial graph**, denoted $M(G)$, is defined as follows. Every edge in G corresponds to a vertex in $M(G)$. For each face in G, an edge e occurs between two vertices in $M(G)$ if the corresponding edges are incident.

(a) Graph G. (b) The medial graph $M(G)$.

Figure 3.2.8: A graph and its medial graph.

Figure 3.2.8 shows a graph and its medial graph. At their core, medial graphs exchange the roles of vertices, edges, and faces. Left-right walks help us identify these new interactions. We discuss the implications of left-right walks on the medial graph later in this section. Thus far, we have taken any planar graph and constructed its medial graph, using left-right walks as the method. That being said, can we "deconstruct" the medial graph into its original graph? Naturally, there is a way, which is known as constructing the inverse medial graph, which we define below.

Definition 3.2.8. Given a 4-regular planar graph Γ, we define the inverse medial graph of Γ, denoted $IM(\Gamma)$, as follows. Select a face color C. Each C-colored face in

Γ corresponds to a vertex in $IM(\Gamma)$, and there exists an edge between two vertices in $IM(\Gamma)$ if the corresponding faces in Γ share a vertex.

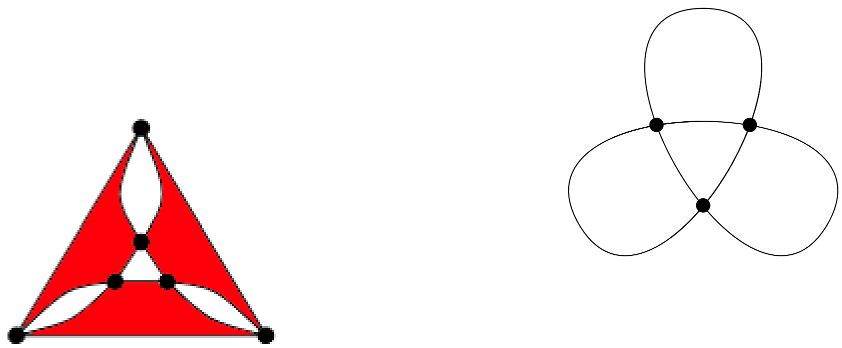

(a) 4-regular graph Γ, with perfect 2-face coloring. (b) The inverse medial graph $IM(\Gamma)$ using red faces.

Figure 3.2.9: A graph and one of its inverse medial graphs.

We see a graph and its inverse medial graph in Figure 3.2.9. Mirroring medial graphs, inverse medial graphs also interchange the roles of vertices, edges, and faces in a graph. Naturally, the interactions of the inverse medial graph counteract those of the medial graph. Thus, unsurprisingly, the inverse medial graph of a medial graph is the original graph, and the medial graph of an inverse medial graph is also the original. In other words, one construction is the inverse of the other.

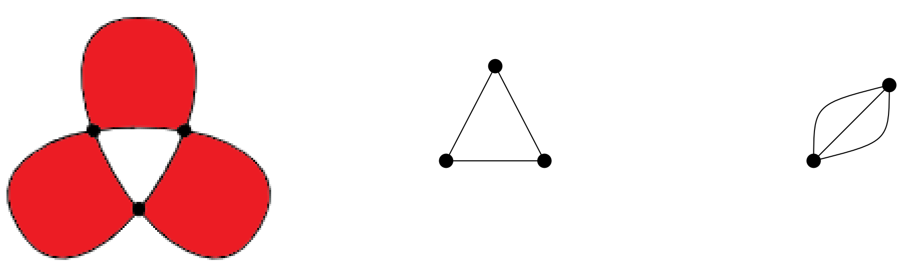

(a) A 4-regular graph G with faces colored. (b) $IM(G)_R$ based on red-colored faces. (c) $IM(G)_W$ based on the white-colored faces.

Figure 3.2.10: Two different inverse medial graphs for a graph G.

One final note on inverse medial graphs is determining which face coloring to consider. Since the initial graph is 2-face colorable, there are two possible inverse medial graphs that can result from this process. Because of this, we specify which color is used to derive the inverse medial graph by including a subscript C, referring to the face color C. Figure 3.2.10 shows the two variations on the inverse medial graph of a 4-regular graph G. Note the statement in previous paragraph still holds: regardless of which face color we choose in constructing the inverse medial graph from G, applying the medial graph process to this graph will always result in returning to this original graph, G—though possibly in different planar orientations.

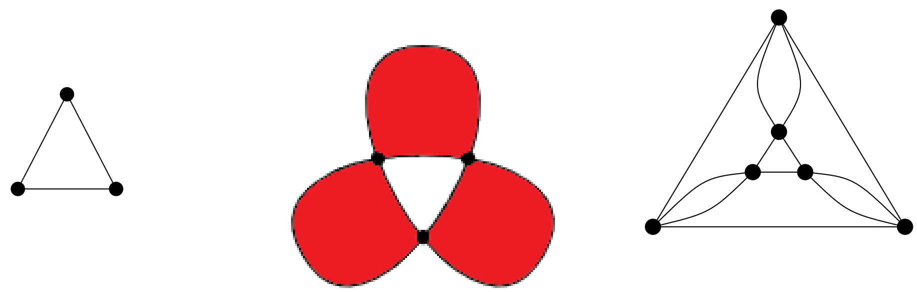

(a) Inverse medial of G, $IM(G)_R$. (b) A 4-regular graph G with faces colored. (c) The medial graph of G, $M(G)$.

Figure 3.2.11: $IM(G)$, G, and $M(G)$.

Consider the three graphs in Figure 3.2.11, which shows the inverse medial graph, an original graph, and the medial graph. When traversing any of these three derivations of graphs seen in Figure 3.2.11, we have numerous options at each vertex to create a walk. Our choice at each step, however, impact the overall walk. The goal of traversing the graphs is to ensure we encounter each edge once. In order to traverse the graphs in this manner, we travel these graphs using straight Eulerian cycles.

Definition 3.2.9. In a graph, if a cycle uses every edge of the graph at most once, the cycle is called an **Eulerian cycle**. Should the cycle use each edge exactly once, then we call the cycle an **Eulerian tour**. In an even-regular graph, Eulerian cycles (tours) are considered **straight** if the cycle (tour) leaves a vertex by the opposite edge from which it entered.

Straight Eulerian cycles are only applicable in even graphs, where we have a notion

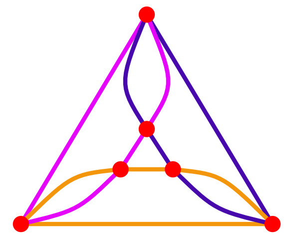

Figure 3.2.12: Figure 3.2.7c with straight Eulerian cycles denoted.

of an "opposite" edge, even if the orientation does not indicate edges are opposite another. Using straight Eulerian cycles, we can easily travel through a shadow graph (since it's 4-regular) and identify the knots in its respective link. Additionally, should a graph be traversable via a straight Eulerian tour—so it is comprised of just one Eulerian cycle—we can topologically interpret the graph as a knot. Figure 3.2.12 denotes the graph from Figure 3.2.7c with its three straight Eulerian cycles. Recall, in Figure 3.2.7b, we identified three separate left-right cycles and, unsurprisingly, the three left-right cycles correspond to the three straight Eulerian cycles. From [9], we have the following bijection:

Lemma 3.2.10 ([9])**.** *Let G be a connected planar graph and let K be its medial graph. Then there is a bijection between straight Eulerian cycles in K and left-right cycles in G.*

This lemma will be extremely useful in determining whether or not a *kōlam* is monolinear, the overall goal of this research and one indicator of *latshanam* drawings. In the next chapter, we utilize these graph theoretic ideas to interpret the ritual art form mathematically.

Chapter 4

Mathematical *Kōlams*

With our understanding of *kōlam* and graph theory, we now form the connection between these two topics. First, we will rigorously define how to construct any *kōlam*. In this process we clarify mathematical ways in which we can perceive the art. We then define the idea of barriers and use them to identify variations among the drawings. Finally, in the pursuit of culturally more significant drawings, we find a few ways in which we can achieve two goals: identifying if a *kōlam* is monolinear and determining ways to draw a monolinear *kōlam*.

4.1 Drawing a *Kōlam*

In Chapter 2, we discussed the Tamil perspective to drawing a *kōlam*, and although the method to construct them may seem innate to most Tamil women, others may struggle with the construction. In the hope of creating monolinear *kōlam*, we mathematically show a way to draw some labyrinthine designs. Because of this, we start at the very beginning, choosing where to place the *pulli*. For the remainder of this work, we assume that n is an odd positive integer.

Definition 4.1.1. An n-***pulli*** **pattern** is an arrangement of points in the Cartesian plane with coordinates (x, y), such that $|x| + |y| \leq n - 1$, for even integers x and y.

We can see an example of what this looks like in Figure 4.1.1 where $n = 5$. The *pulli* will always be denoted in red. Looking closer at this *pulli* pattern, we notice that the number of dots in both the rows and the columns follows the pattern $1, 3, 5, 3, 1$, forming in a diamond-like shape. In general, for any n-pulli pattern, the number of *pulli* in both the rows and columns follow the pattern $1, 3, \ldots, n-2, n, n-2, \ldots, 3, 1$ and, moreover, there are exactly n *pulli* in both the central row and central column of the design. Thus, using basic counting techniques, we can count the total number of *pulli* in any given pattern, which is $\frac{n^2+1}{2}$.

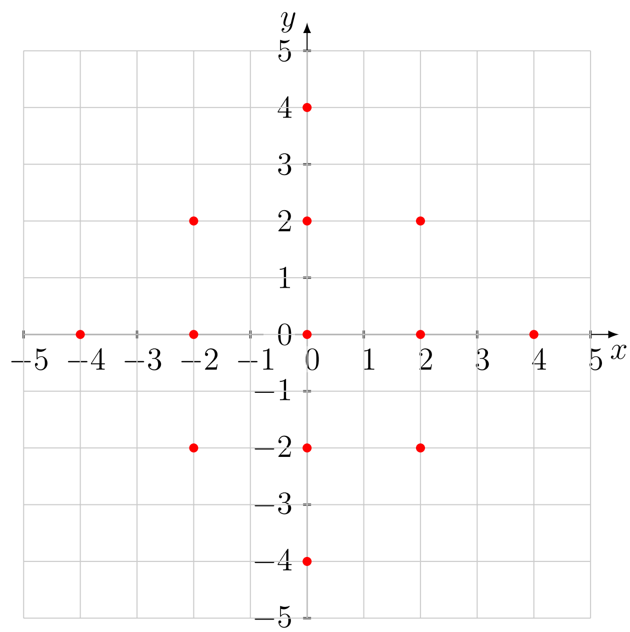

Figure 4.1.1: An $n = 5$ *pulli* pattern over the Cartesian plane.

Once we have created a *pulli* pattern, we are free to begin making a *kōlam*. We can draw any arbitrary *kōlam*, so long as we adhere to the *Kōlam* Crafting Rules outlined in Rule 2.3.1. However, to understand the process of drawing, we start by drawing what we refer to as a "dense" *kōlam*.

Rule 4.1.2 (Dense *Kōlam* Drawing)**.** For $n \geq 3$, to create a dense *kōlam*, we follow these steps:

1. Construct an n-*pulli* pattern according to Definition 4.1.1.

2. Place the drawing instrument at $(0, n)$.

3. Draw from $(0, n)$ to $(0, n-2)$, tracing the left-half of a downward facing teardrop. Then draw the line segment from $(0, n-2)$ to $(n-2, 0)$.

4. Draw the lower-half of a left-facing teardrop from $(n-2, 0)$ to $(n, 0)$. Complete the teardrop to $(n-2, 0)$.

5. Draw a line segment from $(n-2, 0)$ to $(0, -(n-2))$. Create a right-facing teardrop, curving up and left to $(-n, 0)$ and down and right back to $(-(n-2), 0)$.

6. Trace the line segment from $(-(n-2), 0)$ to $(0, n-2)$. Complete the curve by connect to the starting point by drawing the right side of the downward facing teardrop. Note the *pulli* at $(n, 0)$, $(0, n)$, $(-n, 0)$, and $(0, n)$ are circumscribed by the teardrops.

7. Move the drawing instrument to the point $\left(\frac{3}{2}, n - \frac{5}{2}\right)$. Draw a semicircle of radius $\frac{\sqrt{2}}{2}$ around $(2, 2)$ to the point $\left(\frac{5}{2}, n - \frac{7}{2}\right)$. Draw the side of a stadium from $\left(\frac{5}{2}, n - \frac{7}{2}\right)$ to $\left(-\left(n - \frac{7}{2}\right), -\frac{5}{2}\right)$.

8. Draw a semicircle of radius $\frac{\sqrt{2}}{2}$ from $\left(-\left(n - \frac{7}{2}\right), -\frac{5}{2}\right)$ to $\left(-\left(n - \frac{5}{2}\right), -\frac{3}{2}\right)$. Complete the stadium by drawing from $\left(-\left(n - \frac{5}{2}\right), -\frac{3}{2}\right)$ to $\left(\frac{3}{2}, n - \frac{5}{2}\right)$.

9. Repeat Steps 7 and 8, drawing a stadium starting at the points located at each $\left(2k - \frac{1}{2}, n - 2k + \frac{1}{2}\right)$, where $1 \leq k \leq \frac{n}{2}$, $k \in \mathbb{Z}$. The last line drawn will start at the point $\left(n - \frac{7}{2}, \frac{5}{2}\right)$. When drawing each stadium, the edge on the lower right side will start in Quadrant I and end in Quadrant III. Likewise, the other edge travels the opposite direction.

10. Repeat steps 7–9 starting in the Quadrant II of the Cartesian plane, beginning at the point $\left(-\frac{3}{2}, n - \frac{5}{2}\right)$. The last line drawn will start at the point $\left(-\frac{7}{2}, \frac{5}{2}\right)$, and

all *pulli* should be circumscribed by the desired shapes mentioned in Rule 2.3.1. Similar to the previous stadiums, the lower-left edge of each stadium begins in Quadrant II and ends in Quadrant IV. The other edge follows the opposite direction.

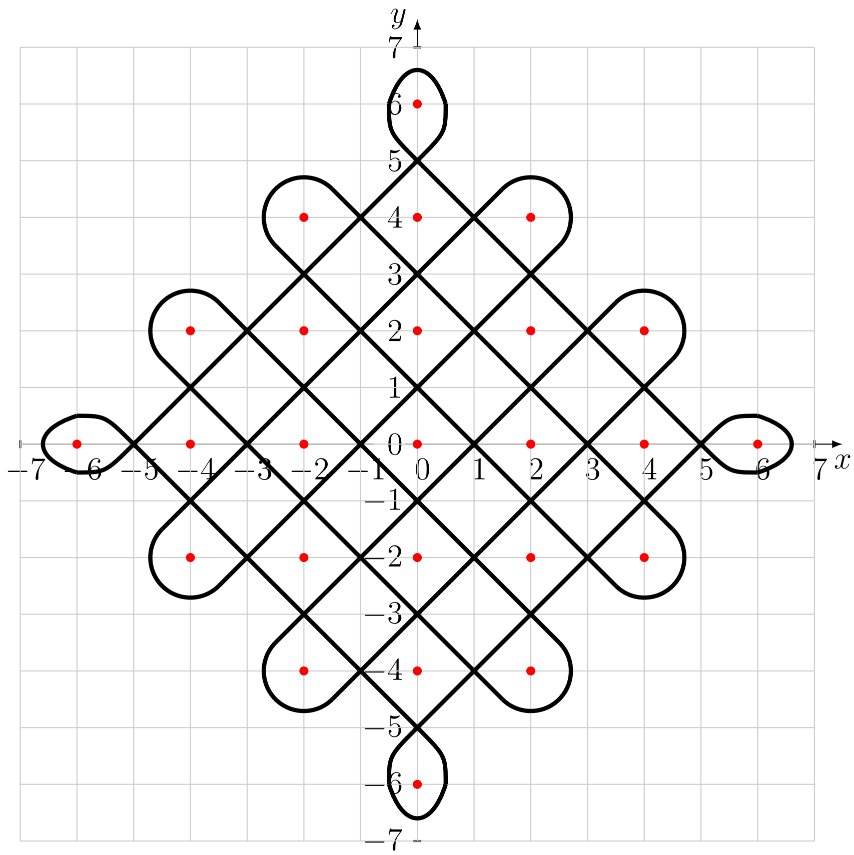

Figure 4.1.2: Picture of a dense *kōlam* for $n = 7$, using Rule 4.1.2.

Figure 4.1.2 shows the dense *kōlam* of a 7-*pulli* pattern. Following the rules for drawing, we can see that this figure is a link diagram comprised of five knots. While in this figure we include the axes and grid, they are usually omitted. Because of this, we will only draw *pulli* and *kodu*—dots and lines—for the remainder of this work.

In addition to our stipulation of n being an odd integer, we add one more restriction upon n: $n > 3$. Figure 4.1.3 shows why we omit the *kōlams* drawn on the 1-*pulli* and 3-*pulli* patterns. The only possible *kōlam* on a 1-*pulli* pattern is simply a circle, and in a 3-*pulli* pattern, the dense *kōlam* is compristed of a square with four teardrops, one at each of the corners. Since these are the only *kōlams* on their respective patterns, we focus our work on *pulli* patterns when $n \geq 5$.

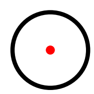

(a) Picture of the *kōlam* on 1-*pulli* pattern.

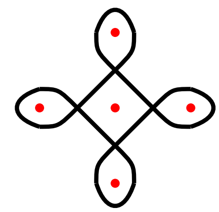

(b) *Kōlam* on 3-*pulli* pattern.

Figure 4.1.3: Two *kōlams* on small *pulli* patterns.

As mentioned in Chapter 2, monolinear *kōlams* are considered more significant than *kōlams* comprised of multiple lines. However, any *kōlam* on $n \geq 5$ *pulli* constructed from the *Dense Kōlam Drawing Rules* 4.1.2 are multilinear. In order to create these shining figures, we need to adjust the “dense” drawings. The way Tamil women create monolinear *kōlams* is by limiting the number of times the lines intersect. Figure 4.1.4 shows a woman working on making a monolinear *kōlam*, and we can see this idea in the design. Consider the lower part of the design compared to the lower part of the dense *kōlam*. We see teardrops in Figure 4.1.4 where the dense *kōlam* has squares. Additionally, we see lenses in the lower half of this partially completed *kōlam*. The way we can interpret creating these different shapes is by restricting the number of crossings, which can be done by placing barriers in the n-*pulli* pattern.

Definition 4.1.3. In an *n-pulli* pattern, a **barrier** b is a vertical or horizontal line segment of length two, centered at non-*pulli* integer points (x, y) such that $|x|+|y| < n$ and either x or y is odd, but not both.

Figure 4.1.5 shows how we can envision barriers in dense *kōlams*. We use a dashed blue line to differentiate between barriers and the *kodu* of *kōlams*, which we color black. Although none of the blue lines drawn in Figure 4.1.5 satisfy the defintion

Figure 4.1.4: Woman drawing a monolinear *kōlam*, [14].

of barriers, as they are all centered where $|x| + |y| = n$, we can interpret them as "external barriers". These external barriers are innate, given from the size of the *pulli* pattern. The external barriers limit the size in the dense *kōlam*, where we create the maximum number of possible crossings. As n will always be finite, each drawing is finite itself, so we only draw external barriers when needed for clarity of interpretation. Even though external barriers always exist, even if the *kōlam* is not dense, Figure 4.1.6 shows what occurs when we place a barrier inside the design.

This idea of a barrier appears in many mathematical works. Jablan [13] discusses mirror curves, segments that lines reflectively bounce away from the mirror should a line touch the curve, which act similarly to barriers. The main difference between mirror curves and barriers is how a line interacts with them. When a line interacts with a mirror curve, the line will continue its trajectory into the mirror, hitting it, and the line bounces off at its supplementary angle with respect to the mirror. When a line approaches a barrier, however, the line curves away from it, never making contact with the barrier itself. A mirror curve's location and orientation implies which direction this supplementary angle turns. The same holds for barriers, although the angle change is not immediate. Chavey [5] shows us a closer description of how barriers work in *kōlam*, since the mirror curves in the *sona* designs of the Tchokwe people

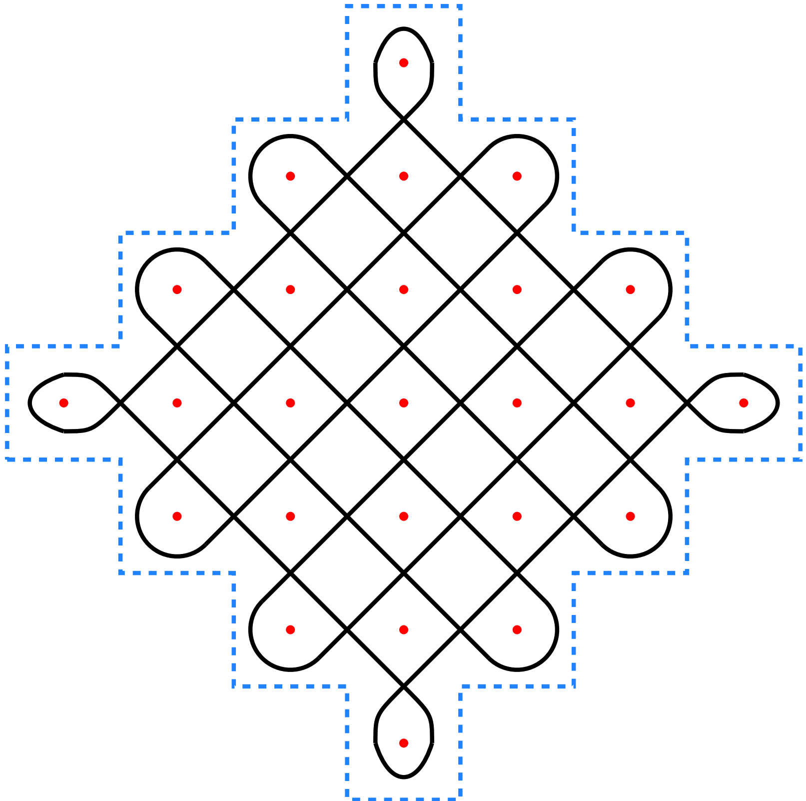

Figure 4.1.5: Dense *kōlam* for $n = 7$ with natural external barriers.

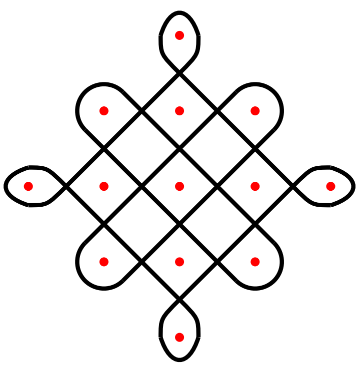

(a) Dense *kōlam* before placing barrier.

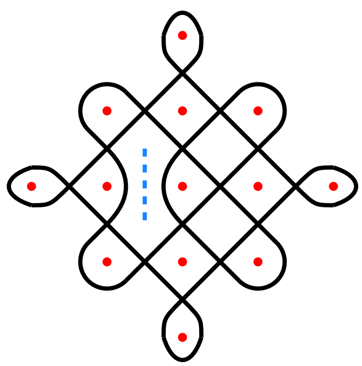

(b) Dense *kōlam* after placing a vertical barrier.

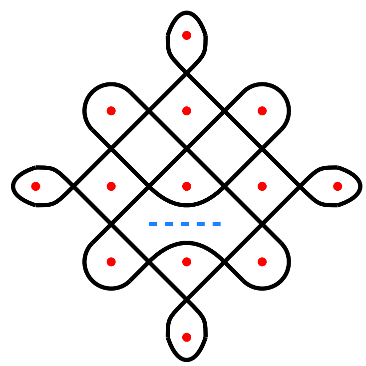

(c) Dense *kōlam* after placing a horizontal barrier.

Figure 4.1.6: The effect of barriers in a dense *kōlam*, for $n = 5$.

work almost identically. The line curves away from the barrier instead of bouncing off of it. The barriers simply alter the way the lines interact with each other, by forcing an edge to travel a new direction.

One vital consequence to note about barriers is where they can be placed. A barrier line segment will always be placed such that the segment starts and ends on x, y coordinates where both values are odd. This means that a barrier will never intersect any *pulli*. However, there are two ways that a barrier can appear, as a vertical line or as a horizontal line. We now identify the two types of barriers, vertical and horizontal.

Definition 4.1.4. Consider an *n-pulli* pattern. A **vertical barrier** b_V is a barrier with midpoint (x, y) such that $|x| + |y| < n$ and x is an odd integer. Similarly, a **horizontal barrier** b_H is a barrier with midpoint (x, y) where $|x| + |y| < n$ and y is an odd integer.

(a) Placing a vertical barrier. (b) Effects of placing a horizontal barrier.

Figure 4.1.7: Placing barriers and its effects.

We see how the vertical and horizontal barriers look and act in Figures 4.1.7a and 4.1.7b. Figure 4.1.8 shows what happens when we insert all possible barriers, including the external barriers, in a 3-*pulli* pattern. We see that the barriers result in a circle being drawn around each *pulli*. This is no rare occurrence. If we place all barriers in any *n-pulli* pattern, we see the same design of circles surrounding each *pulli*.

Considering both *pulli* and barriers, we can now commence a closer investigation on *kōlams* as a whole. We provide a mathematical definition and notation of these designs.

Definition 4.1.5. A ***kōlam***, $\mathcal{K}(n, B)$, is a collection of closed lines over an *n-pulli*

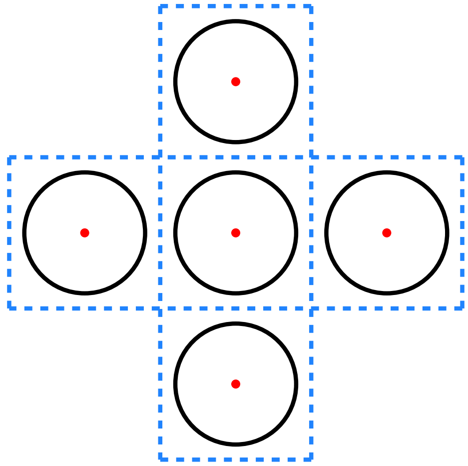

Figure 4.1.8: Resulting *kōlam* from considering all barriers.

pattern using a set of barriers B such that Rule 2.3.1 is maintained. If the *kōlam* is drawn using only one line, then the *kōlam* is considered **monolinear**.

Using this definition of *kōlams*, we pave the way for our overall goal of creating monolinear designs. In order to achieve this goal, we next look at symmetry with barriers. Each drawing should have reflective symmetry. Unless a barrier lies on the $x-$ or the y-axis, introducing just one barrier will break the required symmetry of the *kōlam*. Figure 4.1.9 indicates this, where Figure 4.1.9a shows a single barrier placed on the y-axis, and Figure 4.1.9b depicts a barrier placed away from either axis. Therefore, in situations such as Figure 4.1.9b, we need to carefully insert a second barrier to ensure the design is in fact symmetric. We call this a barrier pair.

Definition 4.1.6. A **vertical pair of barriers** $\beta = (x, y)_X$ is a pair of two barriers with midpoints (x, y) and $(x, -y)$, mirrored across the x-axis. Likewise, a **horizontal pair of barriers** $\beta = (x, y)_Y$ is a pair of two barriers with midpoints (x, y), $(-x, y)$, mirrored across the y-axis.

Figure 4.1.10 shows that the axis of symmetry holds no implication on the direction of the barriers. We can add a vertical pair of vertical barriers or a vertical pair of horizontal barriers, and the *kōlam* will still be symmetric. Notice the ordering of

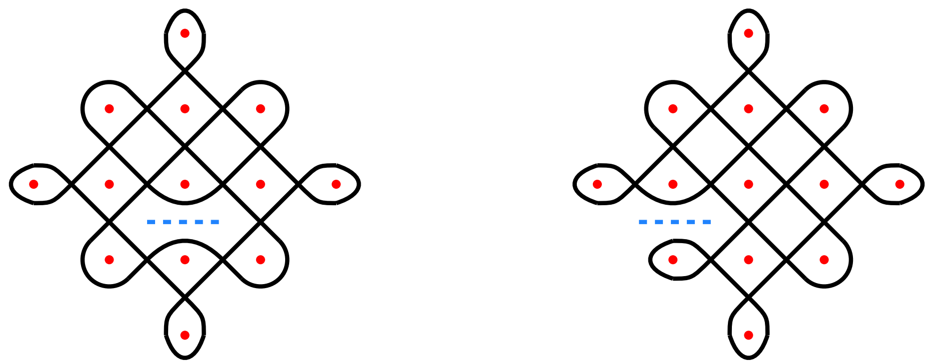

(a) Barrier placement that creates symmetry.

(b) Barrier placement that does not create symmetry.

Figure 4.1.9: Placing one barrier and the resulting symmetry or asymmetry.

(a) A horizontal pair of vertical barriers, $\beta = (1, 2)_X$.

(b) A vertical pair of vertical barriers, $\beta = (-1, -2)_Y$.

(c) A horizontal pair of horizontal barriers, $\beta = (2, 1)_X$.

(d) A vertical pair of horizontal barriers, $\beta = (-2, -1)_Y$.

Figure 4.1.10: Variations in barrier pairs.

words the four examples in Figure 4.1.10 use. When referring to barrier pairs, we first indicate the axis of symmetry, then we identify which direction the barriers themselves are oriented. What if we desired a *kōlam* with both reflective symmetries? That is, can we combine a horizontal pair of barriers with a vertical pair of barriers? In short, we can; however, we must be careful to ensure symmetry for the entire drawing.

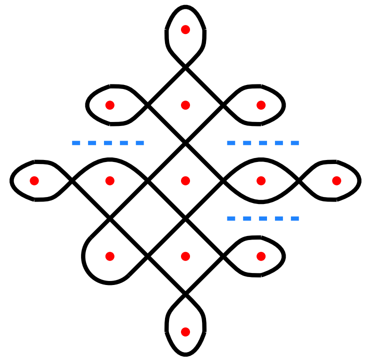

Figure 4.1.11: Drawing of $\mathcal{K}(5, B)$, for $B = \{(2,1)_X, (2,1)_Y\}$.

Examine Figure 4.1.11. A design such as this is why we must proceed with caution. Imagine we folded this *kōlam* along both of its axes of symmetry. We would find that the lower left of the drawing is not symmetric with the other sections. Thus, we cannot have two barrier pairs that share a single barrier, such as the pairs $(2,1)_X$ and $(2,1)_Y$ as seen in the figure. However, we can take two mirrored pairs, such as $(2,1)_X$ and $(-2,-1)_X$ or $(2,1)_Y$ and $(-2,-1)_Y$. We give this union of "mirrored pairs" a name: a quad of barriers.

Definition 4.1.7. A **quad of barriers** $\beta = (x, y)_{XY}$ is a set of four similarly oriented barriers with midpoints $(x, y), (-x, y), (-x, -y), (x, -y)$.

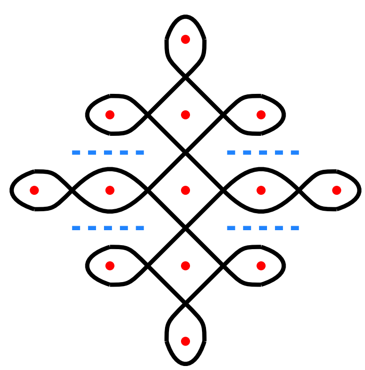

Figure 4.1.12: Drawing of $\mathcal{K}(5, B)$, for $B = \{(2,1)_{XY}\}$.

As noted in Definition 4.1.7, all barriers in a quad of barriers are in the same orientation. That is to say quads of barriers will contain only four horizontal barriers or four vertical barriers. Figure 4.1.12 shows a *kōlam* with a quad of barriers oriented horizontally. We can verify that this drawing satisfies the symmetric requirements of the *Kōlam* Crafting Rules 2.3.1 by "folding" the *kōlam* along both of its axes of symmetry.

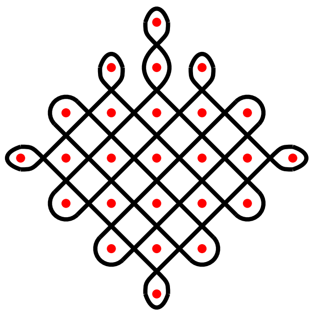

(a) $\mathcal{K}(7, \{(1,4)_X\})$.

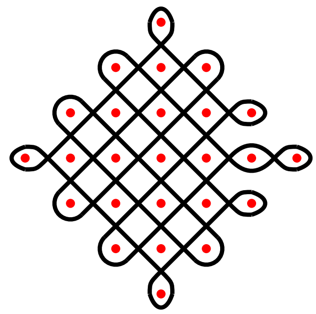

(b) $\mathcal{K}(7, \{(4,1)_Y\})$.

Figure 4.1.13: Two isomorphic *kōlams*.

Since Rule 4.1.2 is specifically for a dense *kōlam*, we include the way to create any *kōlam* $\mathcal{K}(n, B)$, for any *n-pulli* pattern and any set of barriers B.

Rule 4.1.8 (General *Kōlam* Drawing Rules)**.** When drawing any *kōlam* $\mathcal{K}(n, B)$, we follow these steps.

1. Construct an *n-pulli* pattern.

2. Lightly draw each $b \in B$ as a dotted line.

3. Place the drawing instrument at $(0, n)$.

4. Draw from this point as done in Rule 4.1.2.

5. Upon reaching a barrier, trace a continuous curve from the current angle to its supplementary curve, as seen in Figure 4.1.7.

6. Continue tracing lines and following Step 5 when encountering barriers until the line returns to the starting point with the starting angle.

7. If all *pulli* are circumscribed, proceed to Step 10. If not, select a *pulli* at (x, y) that is not fully circumscribed, preferably whose sum $|x| + |y|$ is the largest and in the first quadrant of the Cartesian plane.

8. From the chosen *pulli*, identify the number of adjacent *pulli* one cardinal unit away.

   - If there is 1 *pulli*, draw half of a teardrop facing the adjacent *pulli* that has not already been drawn.
   - If there are 2 *pulli* that form a line containing the chosen *pulli*, draw a curve of a lens in the line that has not yet been drawn.
   - If there are 2 *pulli* that do not form a line with the chosen *pulli*, draw part of a partial stadium that has not been drawn.
   - If there are 3 *pulli*, draw one side of a fan that has not been drawn.
   - If there are 4 *pulli*, draw a side of a diamond that has not been drawn yet.

9. Continue drawing the line as in Rule 4.1.2, reacting to barriers as shown in Step 5. The curve will be finished when the curve arrives to the starting point with the starting angle. Return to Step 7.

10. Erase all barriers. The *kōlam* is complete!

Rule 4.1.8, as well as Rule 4.1.2, can be considered as an algorithm, so these two rules used with barrier sets rotated in 90° intervals will result in isomorphic *kōlams*. With this understanding of barriers and how they impact *kōlams*, consider Figure 4.1.13a, a drawing of $\mathcal{K}(7, \{(1, 4)_X\})$. If we rotate this image 90° clockwise, this will look like Figure 4.1.13b. Although they are drawn differently, we say that these drawings are isomorphic, as they are simply a rotation of each other. Put more generically, any *kōlam* can be rotated in any increment of 90°, leading to unique notations but still providing an isomorphic design. This means that pairs and quads of barriers will be isomorphic if they are rotations of another. Despite this, we must rotate the entire set of barriers of a *kōlam* in order to create an isomorphic drawing. As an example, Figure 4.1.14 shows three separate *kōlams* using similar barrier sets. We can see that two of these are isomorphic, namely Figures 4.1.14a and 4.1.14b. The third *kōlam*, seen in Figure 4.1.14c is not isomorphic to either, since it uses barriers seen in both, making the set of barriers distinct.

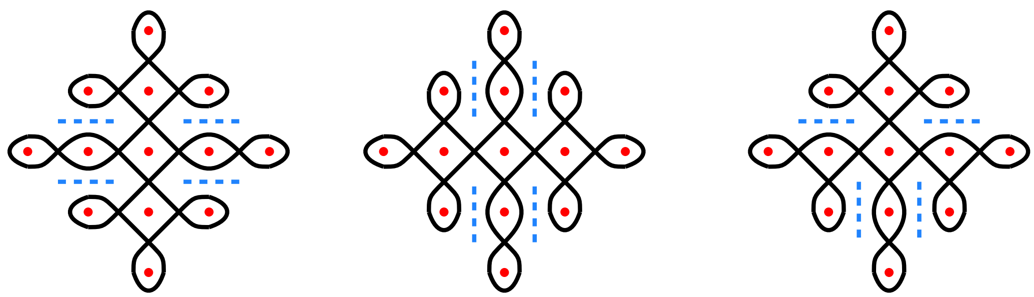

(a) $\mathcal{K}(5, \{(2,1)_{XY}\})$. (b) $\mathcal{K}(5, \{(1,2)_{XY}\})$. (c) $\mathcal{K}(5, \{(2,1)_Y, (-1,-2)_Y\})$.

Figure 4.1.14: Three *kōlams* with differing barrier sets.

Now that we know all the barriers we can place when drawing a *kōlam*, we begin analyzing *kōlam* from a topological graph theory perspective.

4.2 *Kōlams* & Knot Theory

In order to utilize graph theory, we must first identify ways to view *kōlams* as graphs. First, let us consider *kōlams* as links, defined in Definition 3.2.5. Though this is a good start, these are in fact drawings, so we should embed these links in $\mathbb{R}^2$, creating link diagrams, where we ignore any over/underlappings, since *kōlams* do not identify these either. Thus, in addition to Definition 4.2.1, we have a topological definition of *kōlams*.

Definition 4.2.1. A ***kōlam*** $\mathcal{K}(n, B)$ is a link diagram with *pulli* that adheres to the *Kōlam* Crafting Rules 2.3.1.

With this additional definition, we see that *kōlams* are a unique kind of link diagrams, where the *pulli* are also drawn. We can see this, as there is no indication of crossing over or under in the *kōlams*. The only information we can see is that there are crossings. Recall Definition 3.2.6, where we derived a graph from the link diagram. We can do the same with *kōlams*. Given a *kōlam* $\mathcal{K}(n, B)$, we define the shadow graph of $\mathcal{K}(n, B)$, $\mathcal{S}_{\mathcal{K}}(n, B)$, according to Definition 3.2.6; the vertices are located at the crossings of the *kōlam* and edges exist when there is a line in the *kōlam* that connects two crossing without passing through any other crossings. In essence, we remove the *pulli* and insert vertices at crossings. Figure 4.2.1 shows how we transform a *kōlam* into a shadow graph.

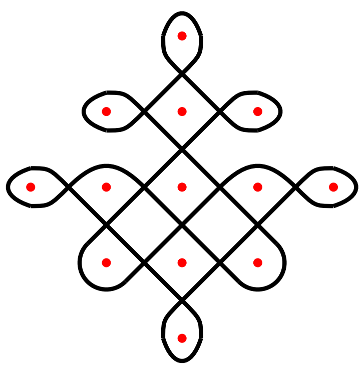

(a) *Kōlam* $\mathcal{K}(5, \{(2, 1)_Y\})$.

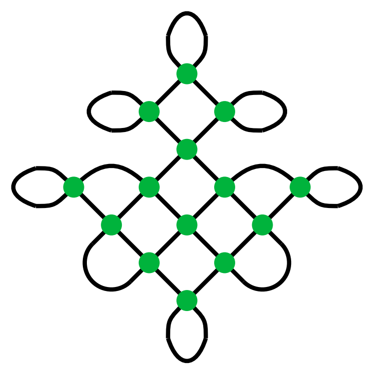

(b) A shadow graph $\mathcal{S}_{\mathcal{K}}(5, \{(2, 1)_Y\})$.

Figure 4.2.1: A *kōlam* and its shadow graph.

When considering the shadow graph of a *kōlam*, we have two major results. The first is that the shadow graph will be 4-regular. We discussed this in Section 3.2.4. As these shadow graphs are 4-regular, we can trace the graphs using straight Eulerian cycles (tours) as mentioned in Definition 3.2.9. Additionally, because of the 4-regular nature of the shadow graphs, we can find a perfect 2-face-coloring of the shadow graph of any *kōlam*. Figure 4.2.2a shows a perfect coloring in red and white for the example in Figure 4.2.1. Note that the outside of the graph is also a face and is colored white. Comparing the face-colored graph with the *kōlam*, we find an interesting discovery here: the *pulli* lie in red faces of the shadow graph in this example. We can choose a perfect 2-coloring of any shadow graph where the red-colored (or white-colored) faces of the shadow correspond with the *pulli* in the *kōlam*. Thus, we can easily derive the inverse medial graph of the shadow graph, notated $IM(\mathcal{S}_{\mathcal{K}}(n, B))$, following Definition 3.2.8. Figure 4.2.2b shows the inverse medial graph of the shadow graph seen in Figure 4.2.2a.

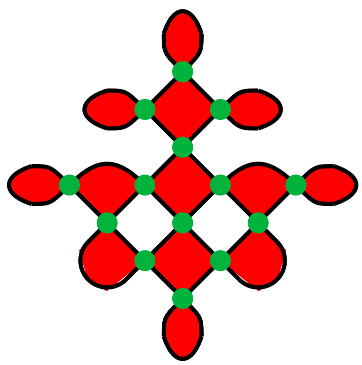

(a) A perfect 2-face coloring of $\mathcal{S}_{\mathcal{K}}(5, \{(2,1)_Y\})$, with 13-red colored faces and 3 white colored faces.

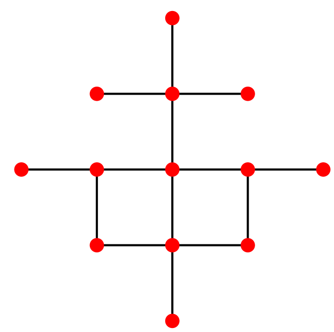

(b) The inverse medial graph of the shadow graph, $IM(\mathcal{S}_{\mathcal{K}}(5, \{(2,1)_Y\}))$, which contains 13 vertices.

Figure 4.2.2: Perfect 2-face coloring and inverse medial graph of a shadow graph.

Similarly, just as we can easily find the inverse medial graph of a shadow graph, we can also reverse the process, starting at a graph and finding its medial graph, following the left-right walk process to derive the medial graph mentioned in Section 3.2.4. Although we can find the medial graph of any graph, not all medial graphs will result in a shadow graph of a *kōlam*; the graph must hold two details in order to result in its medial graph being a shadow graph of a *kōlam*. First, we must have vertices in the orientation of an *n-pulli* pattern. Additionally, all of the graph's edges must connect a vertex to the nearest vertex in a cardinal direction. Figure 4.2.3 shows two graphs. Looking at Figure 4.2.3a, we see a graph that cannot become a *kōlam* after left-right walks, even if the vertices are reoriented in the plane. Among the numerous reasons why, one immediate indication is the three cycle. Any graph that will result in a *kōlam* will contain either no cycles or a cycle of even length greater than or equal to four. This is due to the construction of *pulli* patterns and *kōlams*. Figure 4.2.3b shows a graph that will result in a *kōlam*. Even if a graph will result in a shadow graph of a *kōlam*, we have no immediate indication of whether or not the respective *kōlam* will be monolinear.

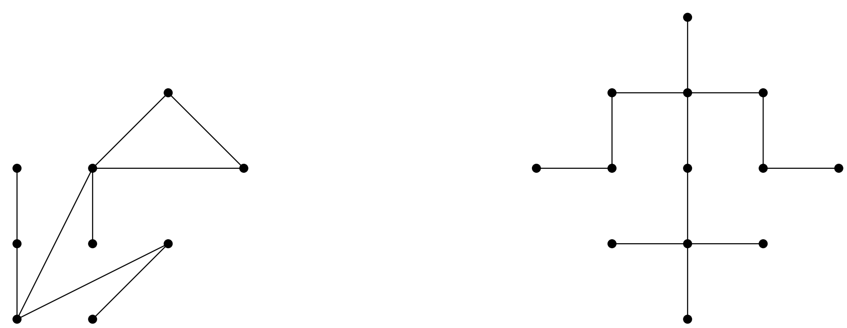

(a) A graph whose medial graph is not the shadow graph of a *kōlam*.

(b) A graph whose medial graph is the shadow graph of a *kōlam*.

Figure 4.2.3: Identifying graphs whose medial graphs are not and are shadow graphs of a *kōlam*.

Recall Lemma 3.2.10. If we have a connected graph and its medial graph, we can determine the number of straight Eulerian cycles in the medial graph from the number of left-right walks in the starting graph. Thus, as shadow graphs are medial graphs depicting *kōlams*, this lemma provides us a direct way of identifying how many straight Eulerian cycles will be in a drawing. We rephrase Lemma 3.2.10 to apply to *kōlams*, using straight Eulerian cycles on the shadow graphs of *kōlams* and the left-right cycles of the inverse medial graphs of said graphs.

Corollary 4.2.2. *Let $IM(\mathcal{S}_{\mathcal{K}}(n,B))$ be an inverse medial graph of a shadow graph $\mathcal{S}_{\mathcal{K}}(n,B)$. Then there is a bijection between the number of left-right cycles in the graph $IM(\mathcal{S}_{\mathcal{K}}(n,B))$ and the number of straight Eulerian cycles used in $\mathcal{S}_{\mathcal{K}}(n,B)$.*

Proof. This follows directly from Definition 4.2.1 and Lemma 3.2.10. $\square$

Recall Defintion 4.2.1, where monolinear *kōlams* contain only one line. Due to the correspondence between *kōlam* and its shadow graph, our objective is to find when a shadow graph contains a straight Eulerian tour. Thus, we have another corollary.

Corollary 4.2.3. *The following are equivalent:*

1. *A kōlam* $\mathcal{K}(n, B)$ *is composed of* ℓ *lines.*

2. *A shadow graph* $\mathcal{S}_{\mathcal{K}}(n, B)$ *contains* ℓ *straight Eulerian cycles.*

3. *The inverse medial of a shadow graph,* $IM(\mathcal{S}_{\mathcal{K}}(n, B))$*, results in* ℓ *left-right cycles.*

Proof. This proof is a direct conclusion of Corollary 4.2.2 and Definition 4.2.1. □

As we proceed, we aim to determine whether a given *kōlam* is monolinear, then we seek to create monolinear *kōlam* using blocks.

4.3 Blocks and *Kōlam* Monolinearity

We provide theorems discussing when a *kōlam* is monolinear. In order to get there, we first identify issues when determining whether a *kōlam* is monolinear. The most logical way of finding the number of lines in a *kōlam* – and thereby checking if the *kōlam* is in fact monolinear – is by tracing the design according to its construction. However, as we are provided with a larger number of *pulli*, such as the 100,000 *pulli* example, [14], this can become easily cumbersome, tedious, and time-consuming. Consider tracing the two examples in Figure 4.3.1. In Figure 4.3.1a we see there are three lines comprising $\mathcal{K}(5, \{(1, 0)_Y\})$, and Figure 4.3.1b shows $\mathcal{K}(5, \{(1, 0)_Y, (1, 2)_Y\})$ is monolinear. How can we quickly deduce the number of lines needed to create a larger drawing? The answer starts in subdividing the given *kōlam*. However as *kōlams* themselves are not graphs, we use the shadow graph of the *kōlam*, isolating sections by using blocks.

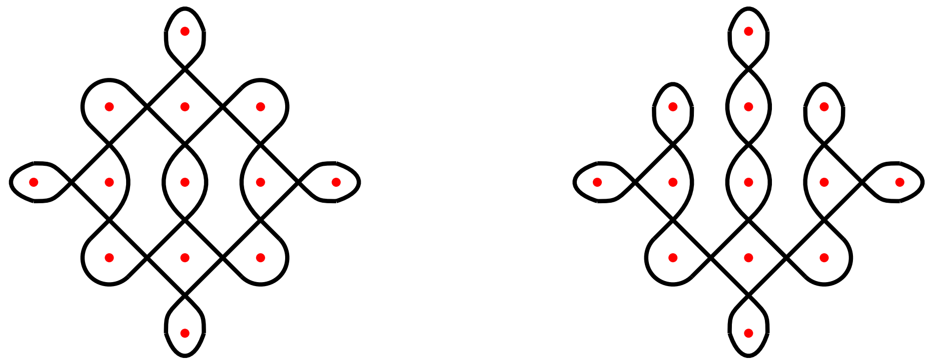

(a) $B = \{(1,0)_Y\}$. (b) $B = \{(1,0)_Y, (1,2)_Y\}$.

Figure 4.3.1: Two variants of $\mathcal{K}(5, B)$, for two different B.

Recalling Definition 3.1.7, we can identify any blocks within the shadow graph of a *kōlam*. In order to find these blocks, we must identify the maximally connected subgraphs that don't contain any cut vertices. Then, once we have determined the number of blocks in the shadow graph as well as how the blocks are connected to one another, we can investigate what occurs within each block. Additionally, each cut vertex in the shadow graph will correspond to a cut edge in its inverse medial graph. However, there are some cut edges in the inverse medial graph whose removal isolates only a vertex. As the lone vertex in the inverse medial graph corresponds to an edge in the shadow graph, we can disregard these cut edges of the inverse medial graph. All the other cut edges in the inverse medial graph, however, correspond to vertices shared between two blocks.

To see this notion more clearly, Figure 4.3.2 showcases the monolinear *kōlam* called Brahma's knot, $\mathcal{K}(7, \{(2,3)_{XY}\})$, along with its shadow graph, inverse medial graph, and the blocks comprising its shadow graph outlined in pink. Looking at Figure 4.3.2d, we see that Brahma's knot can be divided into three blocks. If we find the structures in the inverse medial graph that correspond to the blocks of the shadow graph, we see the upper and lower blocks correspond to trees in the inverse medial graph, but the central block corresponds to a cyclic subgraph of $IM(\mathcal{S}_{\mathcal{K}}(7, \{(2,3)_{XY}\}))$. This gives us two types of possible blocks based on the composition of the inverse medial graph of the blocks.

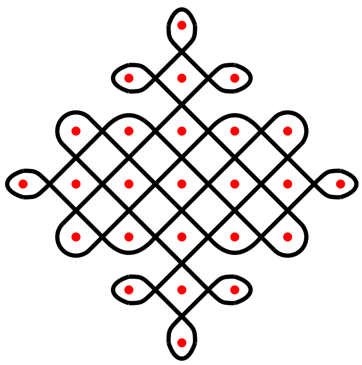

(a) Brahma's knot, $\mathcal{K}(7, \{(2,3)_{XY}\})$.

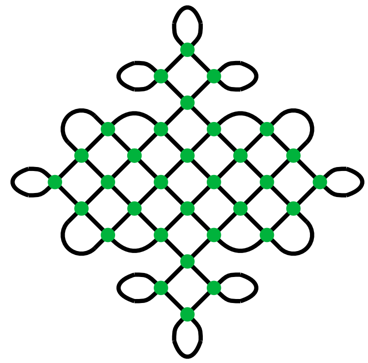

(b) The shadow graph $\mathcal{S}_{\mathcal{K}}(7, \{(2,3)_{XY}\})$.

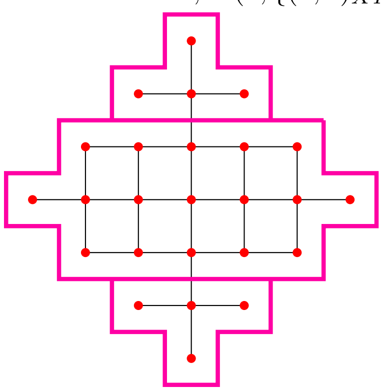

(c) $IM(\mathcal{S}_{\mathcal{K}}(7, \{(2,3)_{XY}\}))$, with the blocks of the shadow graph.

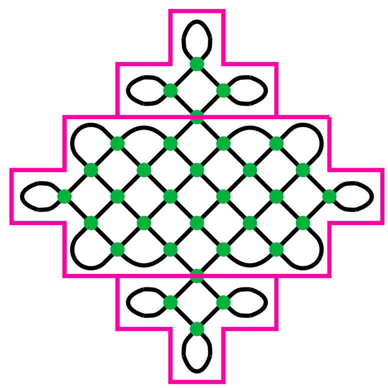

(d) The blocks of $\mathcal{S}_{\mathcal{K}}(7, \{(2,3)_{XY}\})$.

Figure 4.3.2: Blocking process on the Brahma's knot *kōlam*

Definition 4.3.1. Let A be a block in $\mathcal{S}_{\mathcal{K}}(n, B)$. Define $IM(A)$ to be the inverse medial graph of A. That is, $IM(A)$ is the induced subgraph of $IM(S_K(n.B))$ that corresponds to block A in $S_K(n.B)$, removing any edges the connect to vertices outside A. If $IM(A)$ contains a cycle, then A is a **cyclic** block. Otheriwse, A is an **acyclic** block.

As previously mentioned, our categorization of blocks is based on the inverse medial graph. This is because the blocks within shadow graphs always contain cycles, and, while the straight Eulerian cycles in a shadow graph aid us in determining the number of lines needed to construct the associated *kōlam*, they prove to be more challenging to work with when determining monolinearity. Hence, we turn our view of the number of lines in a *kōlam* to the blocks of its shadow graph and the inverse medial graph.

Despite this difficulty, we can trace the shadow graph and its blocks. Should we do this, we find an interesting comparison between the types of blocks. Even though a cyclic block may have more than one straight Eulerian cycle, any acyclic block will always be a straight Eulerian tour.

Theorem 4.3.2. *Any acyclic block A in $\mathcal{S}_{\mathcal{K}}(n, B)$ is composed of exactly one straight Eulerian tour.*

Proof. Let A be an acyclic block in $\mathcal{S}_{\mathcal{K}}(n, B)$ and $IM(A)$ be its inverse medial graph. We use induction on k, the number of vertices in $IM(A)$. If $IM(A)$ only has one vertex, v, then the left-right walk of $IM(A)$ can be written as v or e_v, v, e_v, depending on whether A is the only block of the shadow graph or there is an edge between A and another block, respectively. For the latter of these, we consider the inverse medial graph. As we traverse $IM(A)$, using a left-right walk, the walk e_v, v, e_v can be interpreted as starting at v, using one side of e_v to walk back to v, then walking on the other side of e_v after reaching the vertex. Thus, from Corollary 4.2.3, since $IM(A)$ contains one left-right walk, A is a straight Eulerian tour.

Assume, then, that for any acyclic block whose corresponding inverse medial subgraph has $k \geq 1$ vertices, this block is a straight Eulerian tour. We will show that A is a straight Eulerian tour when $IM(A)$ has $k + 1$ vertices.

Let v be a leaf of $IM(A)$. From the basis step, the left-right walk around v is e_v, v, e_v, a straight Eulerian tour. The inductive step tells us that $A - v$ is also a straight Eulerian tour. Thus, to find a left-right walk of $IM(A)$, we insert the left-right walk e_v, v, e_v where v exists in the cycle of A itself. Thus, the full cycle will be $v_1, e_1, v_2, e_2, \ldots, v_i, e_v, v, e_v, v_i, \ldots, e_{k-1}, v_k, e_{k-1}, \ldots, e_1, v_1$. If we translate this cycle into $IM(A)$, the left-right walk of the inverse medial graph must maintain the alternating nature while still including e_v, v, e_v. That is, if the original walk uses the left side of the edge e_i, it would then use the right side of the next edge. However, since we inserted a straight Eulerian cycle, we first traverse e_v on the right side. After traversing to v, we return along the left side of e_v. Thus, the next edge must be traversed upon its right side. This is the same side the original walk used, so the walk continues as normal, using all edges and vertices. Since this left-right walk uses each side of all edges and each vertex, $IM(A)$ is single left-right walk. By Corollary 4.2.3, A must be a straight Eulerian tour.

Therefore, every acyclic block is a straight Eulerian tour. □

There is a natural corollary from this theorem. Consider a *kōlam* whose only block is acyclic. Since any acyclic block is monolinear, we can see that this *kōlam* is monolinear.

Corollary 4.3.3. *For any kōlam, $\mathcal{K}$, and its inverse medial graph $IM(\mathcal{K})$, if $IM(\mathcal{K})$ is a tree, then $\mathcal{K}$ is monolinear.*

Proof. This proof follows directly from Theorem 4.3.2. □

Unlike their acyclic counterparts, cyclic blocks are not automatically monolinear. We can see this with any $\mathcal{K}(n, \emptyset)$ where $n \geq 5$. Recalling Rule 4.1.2, in order to create the dense *kōlam* $\mathcal{K}(n, \emptyset)$, we create $n-2$ distinct knots. We see that $\mathcal{K}(5, \emptyset)$ contains three knots in Figure 4.3.3a. Additionally, we see $\mathcal{K}(5, \{(2,1)_Y\})$ in Figure 4.3.3b, a monolinear *kōlam*. Below the two *kōlams* we see their respective inverse medial graphs in Figures 4.3.3c and 4.3.3d. Both of these *kōlams* have cyclic blocks in their corresponding shadow graphs, but the designs contain different numbers of lines. One natural way to determine whether or not a cyclic block is a straight Eulerian tour is to simply trace the block. However, this may not always be enough. We provide some conjectures about when a cyclic block will be composed of a straight Eulerian tour.

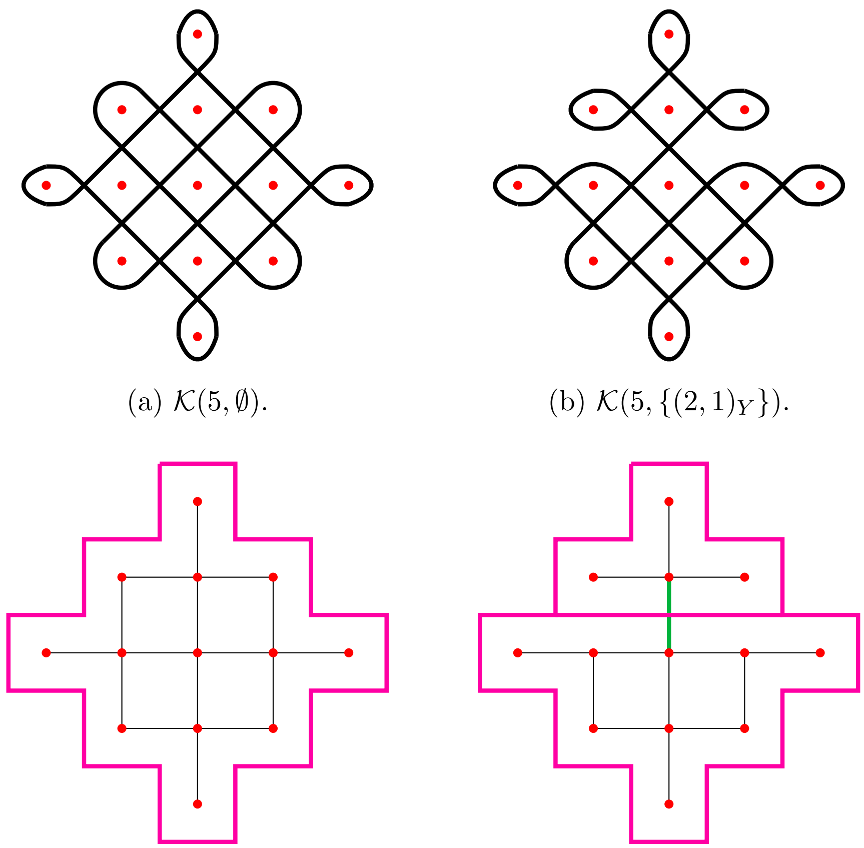

(a) $\mathcal{K}(5, \emptyset)$. (b) $\mathcal{K}(5, \{(2,1)_Y\})$.

(c) $IM(\mathcal{S}_\mathcal{K}(5, \emptyset))$. (d) $IM(\mathcal{S}_\mathcal{K}(5, \{(2,1)_Y\}))$.

Figure 4.3.3: Two *kōlams* with cyclic blocks on top of their inverse medial graphs.

Even though cyclic blocks may or may not be comprised of a straight Eulerian tour, examples previously shown help identify conjectures on when blocks will have this property.

Conjecture 4.3.4. *For a cyclic block A in $\mathcal{S}_\mathcal{K}(n, B)$, A will be a straight Eulerian tour as long as:*

(a) A is an induced subgraph such that it contains all vertices in $\mathcal{S}_\mathcal{K}(n, B)$ corresponding to crossings on the horizontal (or vertical) axis, as well as all vertices above or below (to the left or to the right) of this axis. (See Figure 4.3.3d, for example.)

(b) The largest cycle of IM(A) is equal to $2k$, for an odd natural number k, or

(c) The largest cycle of IM(A) contains paths inside of itself that connect two vertices.

Additionally, we have some intuition on blocks that cannot be a straight Eulerian tour purely based on their inverse medial graph.

Conjecture 4.3.5. *For a cyclic block A in $\mathcal{S}_{\mathcal{K}}(n, B)$, A cannot be a straight Eulerian tour when*

(a) The largest cycle of IM(A) can be drawn as a square with sides of odd length greater than 2,

(b) The largest cycle in IM(A) is a four cycle, or

(c) The only cycle in IM(A) is the boundary, meaning inside the cycle there are only leaves.

We now shift from conversation purely on blocks to the focus of the research – finding when a *kōlam* will be monolinear. The following lemma is needed to show this *latshanam* quality.

Lemma 4.3.6. *Let A_1 and A_2 be two distinct blocks in $\mathcal{S}_{\mathcal{K}}(n, B)$ that share a cut vertex. If A_1 is composed of m_1 straight Eulerian cycles and A_2 is composed of m_2 straight Eulerian cycles, then $A_1 \cup A_2$ is composed of $m_1 + m_2 - 1$ straight Eulerian cycles.*

Proof. Let v be the cut vertex shared by A_1 and A_2. Since $\mathcal{S}_{\mathcal{K}}(n, B)$ is 4-regular and v lies on a cycle in both A_1 and A_2, the degree of v is two in each block and, thus, v lies on one distinct cycle in each block.

Let $v, e_1, u_1, \ldots, u_{i-1}, e_i, v$ be straight Eulerian cycle in A_1 that goes though v and $v, f_1, w_1, \ldots, w_{j-1}, f_j, v$ be the straight Eulerian cycle in A_2 that passes through

v as shown in Figure 4.3.4. To create a straight Eulerian cycle in $A_1 \cup A_2$ passing through v, we may begin at v, traverse from e_1 to u_1 and back up to v via u_{i-1}, e_i, then continue to the opposite edge from e_i, f_1, located in A_2. We then traverse this cycle in A_2, ending with f_j with is incident to v and opposite from edge e_1 where we started. Hence, we have created one straight Eulerian cycle in $A_1 \cup A_2$ from two separate cycles in these blocks. As the remaining cycles were not used in this traversal and A_1 and A_2 share at most one cut vertex by the definition of a block, we now have $m_1 + m_2 - 1$ straight Eulerian cycles in $A_1 \cup A_2$. □

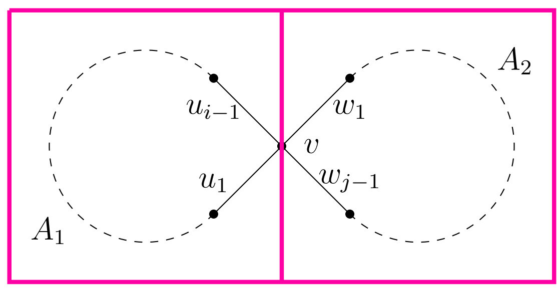

Figure 4.3.4: A cut vertex v shared between two blocks A_1 and A_2.

Note that we may apply this process iteratively, adding another block to the current union of blocks. In each case, the total number of straight Eulerian cycles needed to traverse this subgraph of $\mathcal{S}_{\mathcal{K}}(n, B)$ is one less than the sum needed to traverse the two individual subgraphs. Thus, if we were to take the union of all blocks—i.e., the entire shadow graph itself—the number of straight Eulerian cycles will be equal to the number of cycles within each block minus the total number of blocks plus one. Using this idea, we now have a natural way to identify when a *kōlam* will be monolinear based on its shadow graph.

Theorem 4.3.7. *Given a kōlam $\mathcal{K}(n, B)$ and its shadow graph $\mathcal{S}_{\mathcal{K}}(n, B)$, $\mathcal{K}(n, B)$ is monolinear if and only if for each block A in $\mathcal{S}_{\mathcal{K}}(n, B)$, A is a straight Eulerian tour.*

Proof. We prove the sufficiency of the statement by contraposition. Let $A_1, A_2, \ldots, A_\ell$ be the blocks in $\mathcal{S}_{\mathcal{K}}(n, B)$ such that each block A_i is composed of m_i straight Eulerian cycles, $1 \leq i \leq \ell$. Without loss of generality, assume $m_1 > 1$. By repeating application of Lemma 4.3.6, the total number of straight Eulerian cycles in $\mathcal{S}_{\mathcal{K}}(n, B)$ is $m_1 + m_2 + \cdots + m_\ell - \ell + 1$. Since $m_1 > 1$, $m_1 + m_2 + \cdots + m_\ell \geq \ell + 1$. Therefore, $m_1 + m_2 + \cdots + m_\ell - \ell + 1 \geq (\ell + 1) - \ell + 1 = 2$. Hence, $\mathcal{S}_{\mathcal{K}}(n, B)$ is not a straight Eulerian tour, and consequently $\mathcal{K}(n, B)$ is monolinear.

We now prove the necessity of the statement. Let each block $A_i \in \mathcal{S}_{\mathcal{K}}(n, B)$, $1 \leq i \leq \ell$ be a straight Eulerian tour, and assume that $\mathcal{K}(n, B)$ is not monolinear. Since there are ℓ blocks in $\mathcal{S}_{\mathcal{K}}(n, B)$, all of which are straight Eulerian tours, repeated applications of Lemma 4.3.6 tells us the number of straight Eulerian cycles in $\mathcal{S}_{\mathcal{K}}(n, B)$ is $\ell - \ell + 1 = 1$. Thus, $\mathcal{S}_{\mathcal{K}}(n, B)$ is a straight Eulerian tour and, moreover, by 4.2.3, $\mathcal{K}(n, B)$ is a monolinear *kōlam*, contradicting our assumption. Hence, $\mathcal{K}(n, B)$ is monolinear iff for each block A in $\mathcal{S}_{\mathcal{K}}(n, B)$, A is a straight Eulerian tour.

□

Simply put, when we divide any shadow graph of a *kōlam* into blocks, if each of those blocks is monolinear, then the entire drawing is monolinear, and vice versa. Naturally, we must determine when a block is a straight Eulerian tour. To motivate this, consider Figure 4.3.5. We see $\mathcal{S}_{\mathcal{K}}(7, \{(1,2)_Y, (1,4)_Y\})$ split into its five blocks. Tracing each individual block inside of the boundary, we find that each of the blocks is made of a straight Eulerian tour, which means that the *kōlam* is monolinear. We can cement this by tracing the drawing as we normally would; the *kōlam* $\mathcal{K}(7, \{(1,2)_Y, (1,4)_Y\})$ is monolinear. Additionally, we can identify the inverse medial graph of the associated shadow graph of this *kōlam*. Thus, we can see four of the five blocks are acyclic blocks, which automatically indicate that each is a straight Eulerian tour. The remaining block, a cyclic block, happens to be monolinear. But what if this cyclic block wasn't monolinear? In the next section, Section 4.4, we provide ways to edit a cyclic block so that the block will contain a straight Eulerian tour

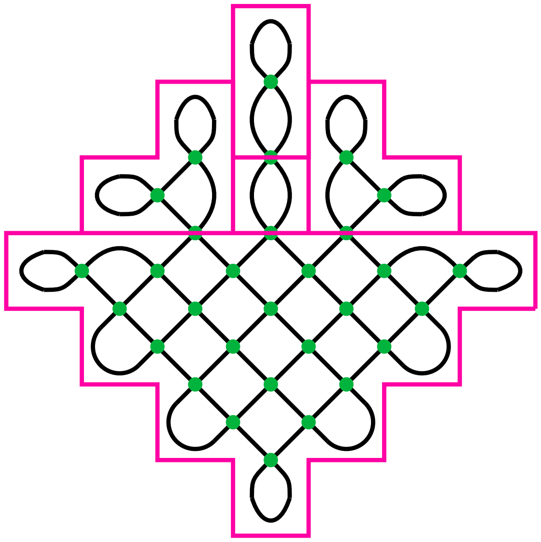

(a) $\mathcal{S}_{\mathcal{K}}(7, \{(1,2)_Y, (1,4)_Y\})$ and the blocks.

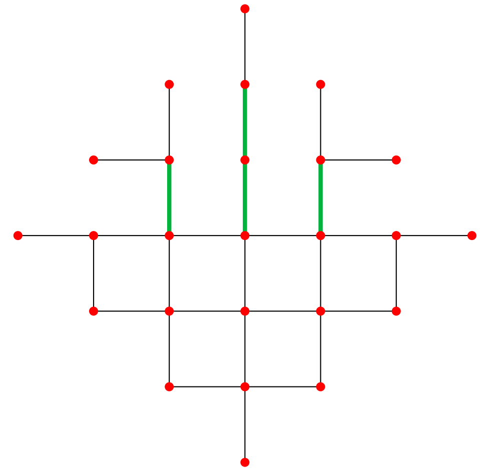

(b) $IM(\mathcal{S}_{\mathcal{K}}(7, \{(1,2)_Y, (1,4)_Y\}))$.

Figure 4.3.5: $\mathcal{S}_{\mathcal{K}}(7, \{(1,2)_Y, (1,4)_Y\})$, its blocks, and the inverse medial graph.

4.4 Monolinear Cyclic Blocks

The first step in deciding whether a cyclic block is a straight Eulerian tour is identifying the number of cycles in the block. Although this may seem counterintuitive, knowing this number can help to adjust the block from being composed of numerous cycles to being a tour, all while still maintaining the block's cyclic nature. We first illustrate this using an example of a shadow graph which includes the *pulli* to strengthen the connection to its *kōlam*.

Observe that Figure 4.4.1 depicts a block containing six straight Eulerian cycles and its inverse medial graph. Note that this block will be unaffected by symmetry, though we will address the necessity of symmetry later. While the proposed block in Figure 4.4.1 can be traversed by straight Eulerian cycles, it is not a straight Eulerian tour as it contains six cycles. Therefore, if the block appeared in the shadow graph of *kōlam* the *kōlam* would not be monolinear. The question arises: How can we adjust a block, like this example, to create a single straight Eulerian cycle?

Consider inserting a path in the inverse medial graph that connects two non-adjacent vertices, say $u, v \in V(IM(A))$. This can be additionally viewed as removing

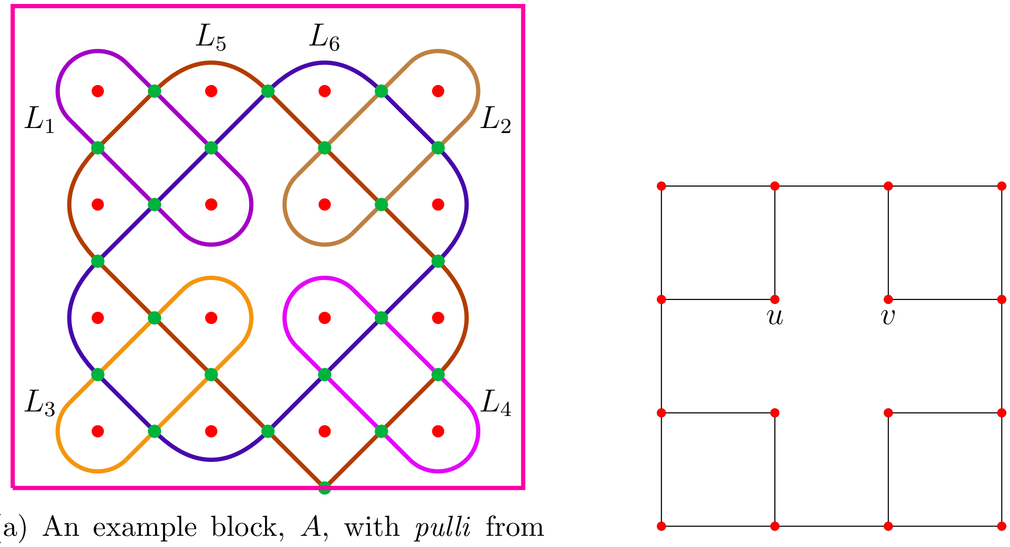

(a) An example block, A, with *pulli* from respective *kōlam*.

(b) $IM(A)$, the inverse medial graph of A.

Figure 4.4.1: A block and its inverse medial graph.

the barrier between the corresponding *pulli* in the *kōlam*. We illustrate an example of this in Figure 4.4.2. Upon a closer investigation, we see that two straight Eulerian cycles from A, specifically L_1 and L_2, merged into the same cycle in the new block A'; we call this new cycle L_{12} as the two distinct cycles combined. The process of inserting an edge in the inverse medial to combine two distinct knots in the block is called inserting an internal *pulli* path.

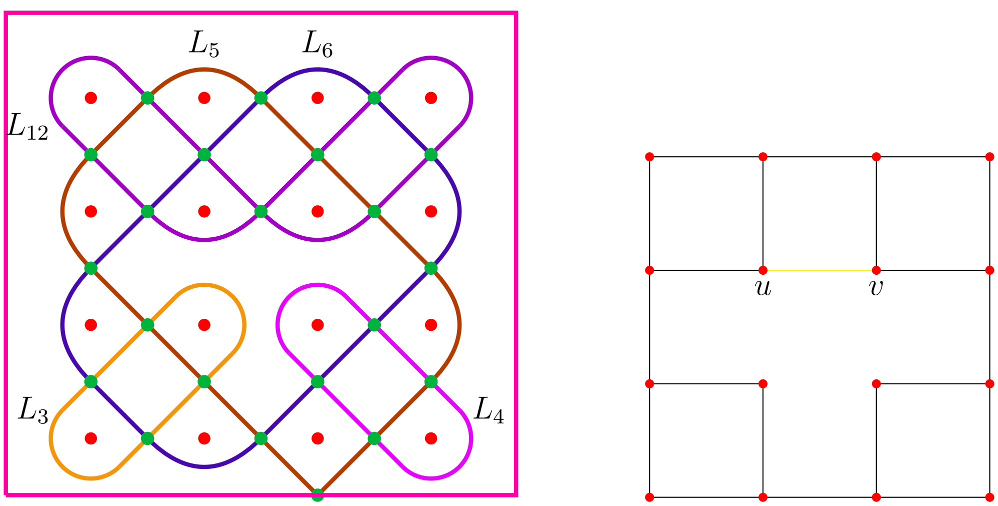

(a) The new block, A', after inserting path.

(b) $IM(A')$, with inserted path in yellow.

Figure 4.4.2: A block and its inverse medial graph after adding new path.

Definition 4.4.1. An **internal *pulli* path** is a path in $IM(A)$ that merges two distinct straight Eulerian cycles in a block A.

As mentioned, an internal *pulli* path inserts a path in the inverse medial graph to connect two nonadjacent vertices. Each path will always be of odd length, to maintain the direction of the new left-right walk of the inverse medial graph. Referring to the previous A', our internal *pulli* path was of length one, and this allowed L_1 and L_2 to become L_{12}. Since we combined two cycles into one, the block in Figure 4.4.2a contains five straight Eulerian cycles. We can repeat this process, hopefully using internal *pulli* paths to combine the remaining five cycles, one at a time. Figure 4.4.3 shows how the block changes after two separate insertions, giving us a total of three internal *pulli* path insertions. Let us try to insert a fourth internal *pulli* path in the inverse medial graph and see how that affects the block.

When attempting to insert this fourth internal *pulli* path, we realize that L_{1234} actually broke apart and became two distinct cycles L_{14} and L_{23}. Conjecture 4.3.5 hints that this fourth insertion would make the block comprised of multiple cycles, as the largest cycle of $IM(A^{(4)})$ is drawn as a 3×3 square.We see this in Figure 4.4.4. This is a key idea of internal *pulli* paths; these paths cannot connect two *pulli* that are in the same straight Eulerian cycle. So, if inserting paths increases the number of cycles, what other operation can we do to instead decrease the number of cycles?

Unsurprisingly, we have another option, one that we have hinted towards in the beginning of this chapter, the use of barriers. Reconsider Figure 4.4.3. In order to make this block monolinear, we must place barriers between two distinct cycles that the same vertex. Figure 4.4.5 shows how placing a single barrier impacts the overall block. Correspondingly in the inverse medial graph, barriers can be interpreted as removing an internal *pulli* path of length one. Similar to inserting internal *pulli* paths, if a barrier is interrupts only one straight Eulerian cycle, the barrier forces the cycle to become two distinct cycles. Thus, we must ensure that any barrier we place lies

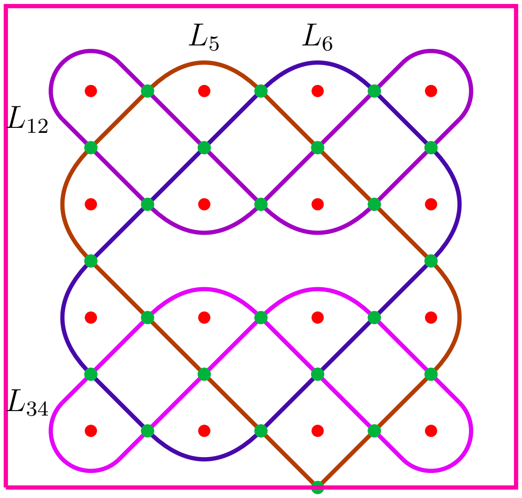

(a) The new block, A''.

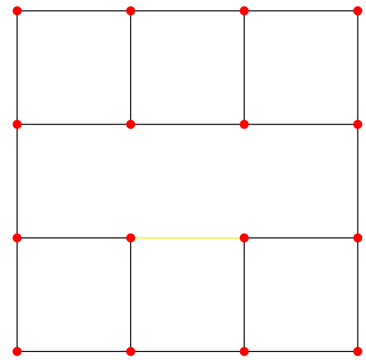

(b) $IM(A'')$, with inserted *pulli* path in yellow.

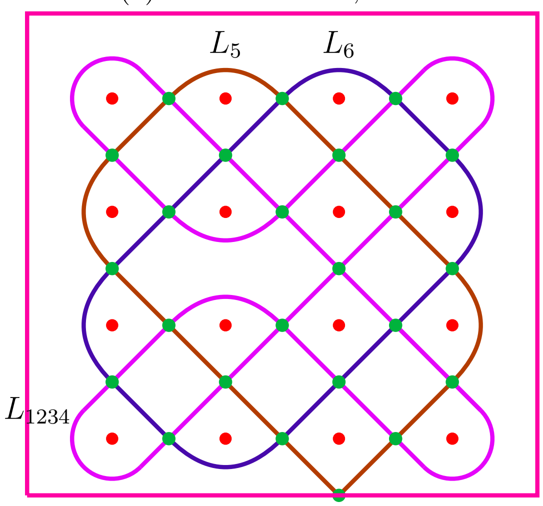

(c) The new block, A''', with a third internal *pulli* path.

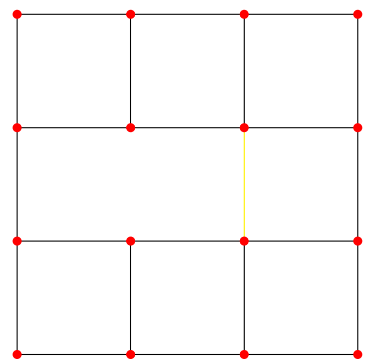

(d) $IM(A''')$, with third internal *pulli* path in yellow.

Figure 4.4.3: Two internal *pulli* paths and their effects on number of straight Eulerian cycles.

on the intersection of two distinct cycles.

Inserting internal *pulli* paths and barriers is all we need to affect the number of straight Eulerian cycles within a block. Thus, we can now turn any cyclic block with more than one Eulerian cycle into a block comprised of a straight Eulerian tour. We summarize the above process in the following algorithm.

Algorithm 4.4.2. Consider a block A that contains more than one straight Eulerian cycle. In order to make A have only one such cycle,

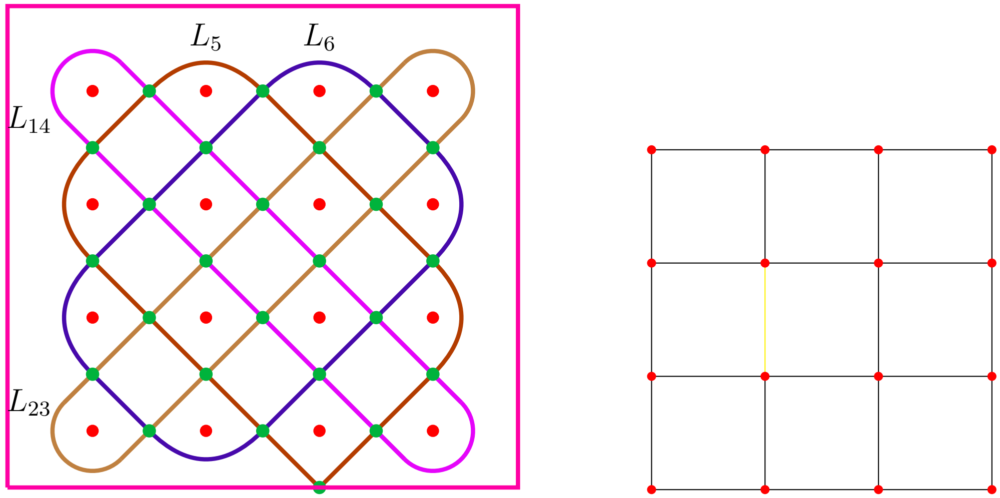

(a) The new block, $A^{(4)}$, with all possible internal *pulli* paths.

(b) $IM(A^{(4)})$, with fourth internal *pulli* path in yellow.

Figure 4.4.4: Effects of internal *pulli* path that connects two vertices in the same knot.

1. Count the number of straight Eulerian cycles of A.
2. Draw the inverse medial graph of A, $IM(A)$.
3. Choose to insert a barrier or an internal *pulli* path.
   - If a barrier is chosen, identify two adjacent vertices in $IM(A)$ to place the barrier between. Remove the corresponding edge.
   - If an internal *pulli* path is to be added, choose two vertices in $IM(A)$ that are odd length apart and whose corresponding *pulli* are inside distinct cycles in the shadow graph, drawing an internal *pulli* path between them.
4. Redraw the block.
5. Recount the number of straight Eulerian cycles in the block.
6. Repeat Steps 2-5 until there is only one cycle in the block, meaning A is a straight Eulerian tour.

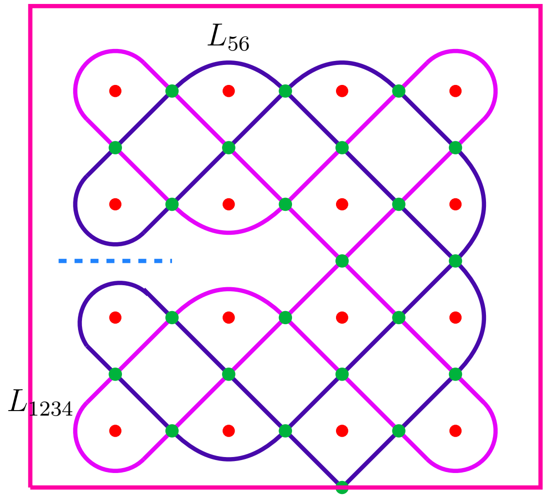

(a) Resulting block $A^{(5)}$ inserting blue barrier.

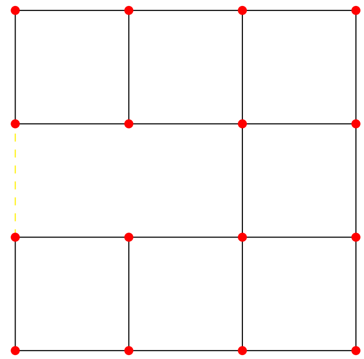

(b) $IM(A^{(5)})$, removing yellow internal *pulli* path.

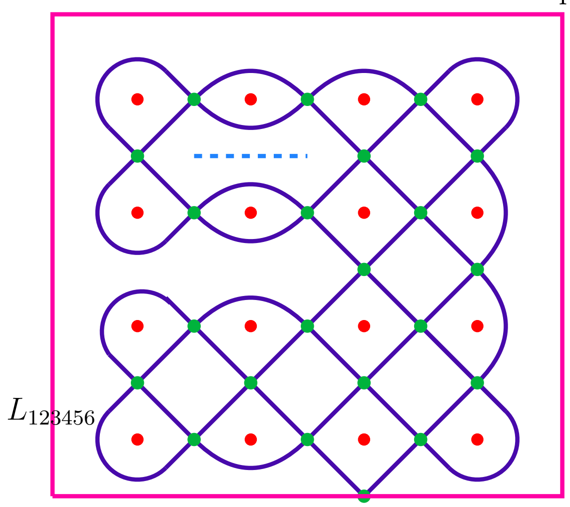

(c) Resulting block $A^{(6)}$ after inserting second barrier.

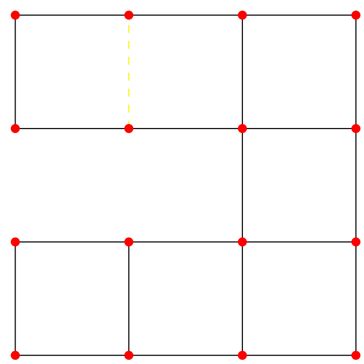

(d) $IM(A^{(6)})$, removing second yellow internal *pulli* path.

Figure 4.4.5: Inserting barriers in a block and its effects.

From this algorithm, the number of times we execute Steps 2-5 will be greater than or equal to the number of knots minus one. We can see this by following the way we made the block in Figure 4.4.1 monolinear. To combine the six knots into one, we inserted three internal *pulli* paths and two barriers, a total of five steps. However, even if each step did not combine two knots, we are not stuck. The algorithm allows us to experiment, creating what we desire, and also helps guide our changes to make our design monolinear. For non-square shaped blocks, this algorithm still works.

Figure 4.4.6a shows a new block D with four straight Eulerian cycles. Note that even though D is not a square, it still does not require internal symmetry. We see two variations in making D a straight Eulerian tour in Figures 4.4.6 and 4.4.7 using the aforementioned algorithm. Note that the choices can be made in any order, as long as the choices are the same; the resulting block will look the same. It is possible to create different blocks if the choices are varied from the original selections.

Up until this point, all blocks we have considered did not need to have internal symmetry. Note that there may be a pair to this block, reflected on the other side of the axis (axes) of symmetry. Thus, when we apply the algorithm to one of the blocks, we must also apply the algorithm to the reflected block. However, not all blocks exist away from the axis (axes) of symmetry. In the construction of some shadow graphs, blocks may exist along or contain an axis (or axes) of symmetry. If a block exists along an axis (or axes), then the block has a mirror adjacent to itself, creating a larger block that contains the axis of symmetry. In either case, we must augment the algorithm. Instead of inserting one internal *pulli* path or one barrier, we must place their reflection as well. To help us understand the algorithm to these kinds of blocks, consider Figure 4.4.8, which contains a block H that needs horizontal symmetry and one way to make H a straight Eulerian tour.

From Figure 4.4.8, we can identify how the algorithm changes. For two straight Eulerian cycles, if they span an the axis of symmetry, either operation—inserting a barrier or internal *pulli* path— must occur on this axis. This is the case is because this augmentation guarantees that the two cycles will combine; if there is an alteration on one side of the axis, there must be another on the other side. This adjustment away from the axis would not guarantee the two straight Eulerian cycles will become one. However, if there is a cycle that doesn't span the axis, this cycle will have a mirror on the other side that will be adjusted at the same time. To see this in action, consider Figures 4.4.8b and 4.4.8c. There are two cycles in Figure 4.4.8b that mirror each other that do not interact with the axis of symmetry. Thus, in Figure 4.4.8c when we combine one of these cycles to the cycle that spans the axis (through the insertion of a barrier), we mirror this action with the reflected cycle, combining three straight Eulerian cycles into one. Regardless of the block composition and adjacency to the axis of symmetry, making a block comprised of a straight Eulerian tour comes down to the aforementioned algorithm. Thus, once all blocks are these tours, we may utilize Theorem 4.3.7 tells us the shadow graph is a straight Eulerian tour, meaning the respective *kōlam* is monolinear.

To create a monolinear *kōlam* of any size, we must go through all the content of this chapter. Our first step is to identify the *pulli* pattern we want. Once we have our desired size, we can consider pairs and quads of barriers that we want. This gives us a natural indication as to how our blocks will be shaped, allowing us to draw each block separately. Recall Theorem 4.3.7. In order to guarantee the *kōlam* we create will be monolinear, we must ensure that each block is a straight Eulerian tour. If a block is acyclic, Theorem 4.3.2 shows us that the block will be a straight Eulerian tour. For any cyclic block, we follow the algorithm to find how to make the block contain a straight Eulerian tour. Once each block is a straight Eulerian tour, we can draw our monolinear *kōlam*, a *latshanam* design.

Graph theory as a mathematical field is often interpreted as a visual topic. We can see interactions between different items or ideas using graph theory. Despite this, the artistic designs of *kōlams* utilize many graph theoretic concepts. Using the ritual art form, we have not only a physical way but also an artistic way of experiencing mathematics. We have found these ties to be innate to both the designs as well as the field of graph theory, which helps us discover ways to quickly determine whether or not any *kōlam* will be monolinear. Dividing each design into its corresponding blocks and analyzing its contents providing a faster approach to this deduction than tracing a large figure. Finding these monolinear designs in and of itself is learning more about the idea of *latshanam*, allowing us to experience the natural beauty within not only art but also mathematics itself.

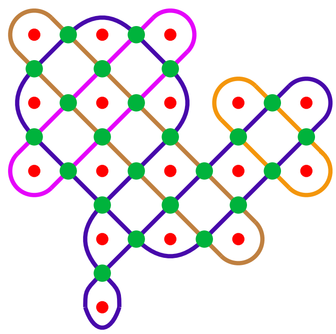

(a) Block D, with *pulli* inserted.

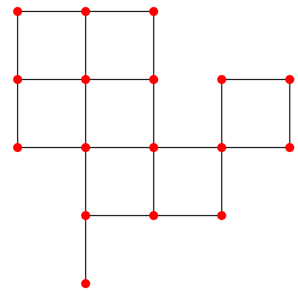

(b) $IM(D)$.

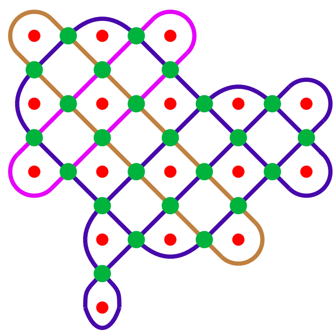

(c) Block D_1', after one step of the algorithm.

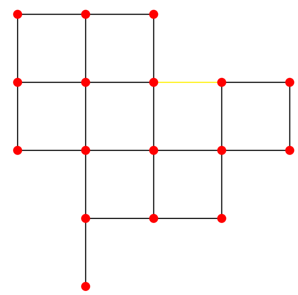

(d) $IM(D_1')$ with yellow edge inserted.

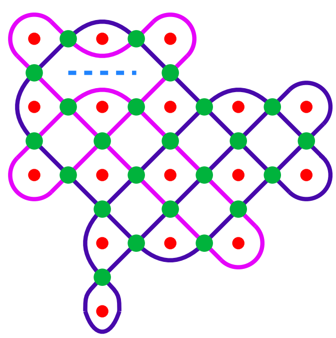

(e) Block D_1'', after a second step of the algorithm.

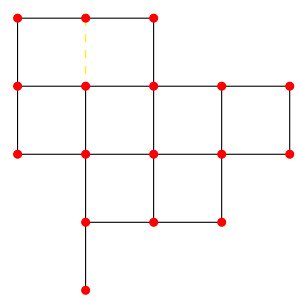

(f) $IM(D_1'')$, with yellow edge removed.

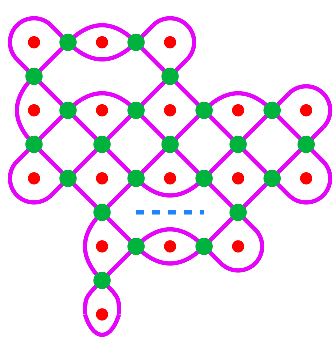

(g) Block D_1''', after a third step of the algorithm.

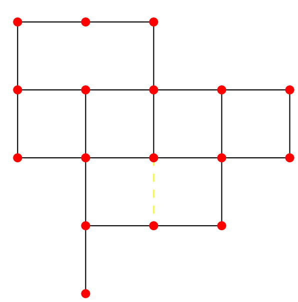

(h) $IM(D_1''')$ with yellow edge removed.

Figure 4.4.6: Making a block D monolinear in one variation.

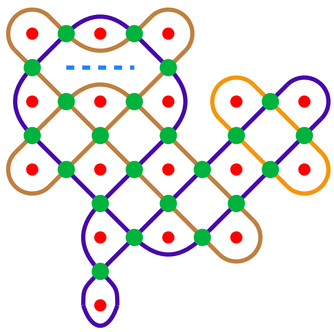

(a) Block D_2', inserting blue barrier.

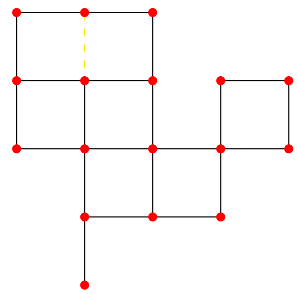

(b) $IM(D_2')$, removing yellow edge.

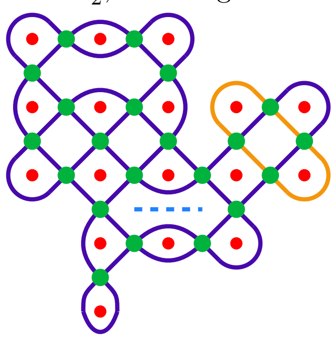

(c) Block D_2'', inserting blue barrier.

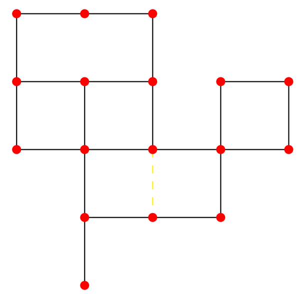

(d) $IM(D_2'')$, removing yellow edge.

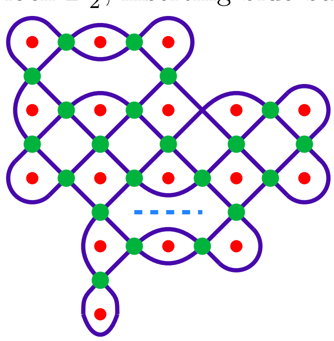

(e) Block D_2''', inserting blue barrier.

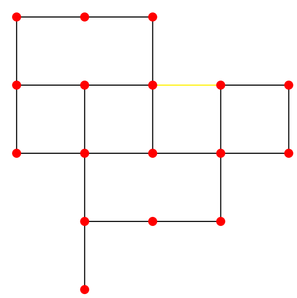

(f) $IM(D_2''')$, inserting yellow edge.

Figure 4.4.7: Making a block D monolinear in a second variation.

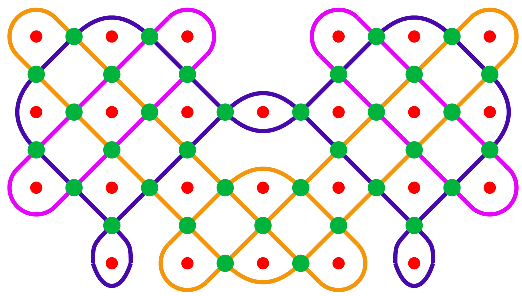

(a) A symmetric block H with *pulli* inserted.

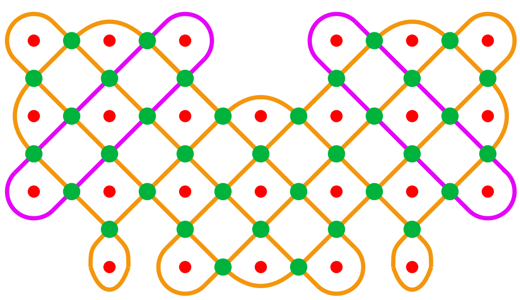

(b) H', the result of inserting an internal *pulli* path.

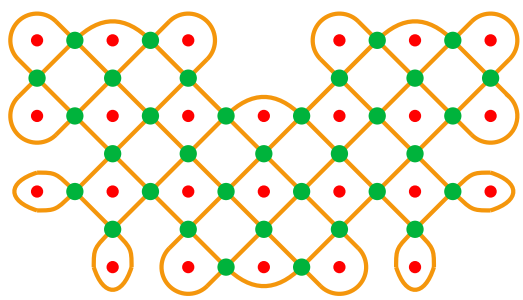

(c) H'', the result of inserting barrier.

Figure 4.4.8: The algorithm on a block requiring symmetry.

References

[1] States and union territories of india. https://en.wikipedia.org/wiki/States_and_union_territories_of_India#/media/File:India\protect\discretionary{\char\hyphenchar\font}{}{}locator\protect\discretionary{\char\hyphenchar\font}{}{}map\protect\discretionary{\char\hyphenchar\font}{}{}blank.svg.

[2] M. Ascher. Graphs in culture: A study in ethnomathematics. *Historia Mathematica*, 15:201–227.

[3] M. Ascher. Graphs in culture ii: A study in ethnomathematics. *Archive for History of Exact Sciences*, 39(1):75–95.

[4] M. Ascher. *Mathematics Elsewhere: An Exploration of Ideas Across Cultures*. Princeton Press, 2002.

[5] D. Chavey. Wallpaper designs of mirror curves inspired by african sona.

[6] D. P. Chavey. Visualizing induction with african sona designs.

[7] J. Connor and N. Ward. Celtic knot theory. *College and University*, 2012.

[8] G. Fisher and B. Mellor. On the topology of celtic knot designs. *Bridges: Mathematical Connections in Art, Music, and Science*, 2004.

[9] C. Godsil and G. Royle. *Algebraic Graph Theory*. Springer, 2001.

[10] V. Gopalan and B. K. VanLeeuwen. A topological approach to creating any pulli kolam, an artform from southern india. *ArXiv*, 30(1-supplement-1):S28–S39, 2015.

[11] J. L. Gross and T. W. Tucker. A celtic framework for knots and links. *Discrete & Computational Geometry*, 46:86–99, 2011.

[12] Y. Ishimoto. Solving infinite kolam in knot theory. *ArXiv*, 22(4):425–460, 2007.

[13] S. V. Jablan. Mirror curves. https://www.mi.sanu.ac.rs/vismath/mir/mir.htm.

[14] V. Nagarajan. *Feeding a Thousand Souls: Women, Ritual, and Ecology in India - An Exploration of the Kolam*. Oxford University Press, 2018.

[15] L. Radovic. Tchokwe sand drawings. — download scientific diagram - researchgate, 2012.

[16] S. Sengupta. *Kolam Tradition in South India: Rangoli in Indian Threshold Design*. D.K. Printworld, Ltd., 2019.

[17] E. Vandendrissche. *String Figures as Mathematics? An Anthropological Approach to String Figure-Making in Oral Tradition Societies*. Springer, 2015.